# Data Summary Report for Fission Product Release Test VI–7

Prepared by
M. F. Osborne, R. A. Lorenz, J. R. Travis, J. L. Collins, C. S. Webster

Oak Ridge National Laboratory
Managed by Martin Marietta Energy Systems, Inc.

Oak Ridge National Laboratory
Oak Ridge, TN 37831–6221

MASTER

# DISCLAIMER

# DISCLAIMER

**Portions of this document may be illegible in electronic image products. Images are produced from the best available original document.**

# Abstract

Test VI-7 was the seventh test in the VI series conducted in the vertical furnace. The fuel specimen was a 15.2-cm-long section of a fuel rod from the Monticello boiling water reactor (BWR). The fuel had experienced a burnup of ~40 MWd/kg U, with inert gas (Kr and Xe) release during irradiation of ~2%. The fuel specimen was heated in an induction furnace for successive 20-min periods at 2000 and 2300 K in a moist air-helium atmosphere. The released fission products were collected in three sequentially operated collection trains designed to facilitate sampling and analysis.

The fission product inventories in the fuel were measured directly by gamma-ray spectrometry, where possible, and were calculated by ORIGEN2. Integral releases were 69% for $^{85}$Kr, 52% for $^{125}$Sb, 71% for both $^{134}$Cs and $^{137}$Cs, and 0.04% for $^{154}$Eu. For the non-gamma-emitting species, release values of 42% for I, 4.1% for Ba, 5.3% for Mo, and 1.2% for Sr were determined. Of the totals released from the fuel, 10% of the Cs, 49% of the Sb, and 98% of the Eu were deposited in the outlet end of the furnace. The total mass released from the furnace to the collection system, including fission products, fuel, and structural materials, was 0.89 g, with 37% being collected on the thermal gradient tubes and 63% downstream on filters. Examination of the thermal gradient tubes showed that large amounts of radiocesium were collected during all three phases of the test, but $^{125}$Sb was collected on the thermal gradient tubes during Phase C only. Posttest examination of the fuel specimen indicated that most of the cladding was completely oxidized to $ZrO_2$, but that oxidation was not quite complete at the upper end. The release behaviors for the most volatile elements, Kr and Cs, were in good agreement with the ORNL Diffusion Model.

# Contents

# Figures

# Tables

# Executive Summary

The objective of this report is to document as completely as possible the observations and results of fission product release test VI-7. This report presents all currently available results for potential use by other reactor safety researchers. Complete interpretation and correlation of the results from earlier tests have been published, and similar data summary reports for previous tests in this project, as well as other reports of related project activities, are listed in the Foreword.

The 15-cm-long fuel specimen, irradiated to a burnup of 40.3 MWd/kg U in the Monticello BWR, contained an initial loading of 112.3 g uranium enriched to 2.87% $^{235}$U. The fission product inventories, as measured in the fuel and calculated by ORIGEN2, and a description of the test procedure and conditions are included in Section 2. The objective of Test VI-7 was to determine the effect of oxidation at high temperature by air and steam on fission product release and transport. Accordingly, the fuel specimen was heated to the test temperatures (2000 and 2300 K) in a moist air-helium atmosphere. The test results and interpretations are presented in Section 3, and these results are compared with data from previous tests in Section 4. The summary and conclusions of this test are included in Section 5, and the references are in Section 6. The most important results are summarized below.

1. Although the Zircaloy cladding had been heavily oxidized during the test, the 15-cm-long fuel specimen had not collapsed but remained standing throughout the test.

2. The values for total fractional release from the fuel specimen, based on ORIGEN2 calculations and gamma ray spectrometry measurements, were ~69% for $^{85}$Kr, 52% for $^{125}$Sb, 71% for both $^{134}$Cs and $^{137}$Cs, and 0.04% for $^{154}$Eu. Other measurement techniques showed that 42% of the I, 4.1% of the Ba, 5.3% of the Mo, and 1.2% of the Sr were released also. About 49% of the released $^{125}$Sb, 10% of the released Cs, and 98% of the released

$^{154}$Eu were deposited on the ZrO$_2$ ceramics at the outlet end of the furnace.

3. The axial distributions of the gamma-emitting fission products in the fuel, as well as the total inventories, were determined by gamma spectrometry. The release fractions from the fuel for $^{125}$Sb, $^{134}$Cs, and $^{137}$Cs were greatest at the bottom end of the specimen and declined with elevation. For $^{154}$Eu, however, for which there was minimal release, the axial distribution remained uniform. The varying releases of Sb and Cs are believed to be related to the extent of oxidation of the UO$_2$.

4. The axial distributions of cesium in the thermal gradient tubes (TGTs) were relatively uniform, with the largest fraction in TGT A. Major peaks of radiocesium were located at 7 to 9 cm (~740°C) and 15 to 20 cm (~550 to 450°C). No other radionuclides were detected in the TGTs except for small concentrations of $^{125}$Sb and $^{60}$Co, both in TGT C.

5. The total mass of deposits on the TGTs and filters was determined by direct weighing to be 0.888 g. Some 37% of this mass was collected on the TGTs, and the remaining 63% was found downstream on connecting tubes and filters, with ~61% of the total release occurring during Test Phase C.

6. Approximately 0.5% of the released iodine (0.33% of the total inventory in the fuel) was collected one of three volatile forms—I$_2$, HI, or CH$_3$I. This fraction of volatile iodine, which is believed to result from the reaction of stable forms such as CsI with impurities in the system, is similar to that observed in most previous tests.

7. The measured diffusion coefficients for the release of $^{85}$Kr and $^{137}$Cs agreed well with previous test results and with the ORNL Diffusion Release Model.

xi NUREG/CR-6318

# Foreword

This document describes the seventh and final test in the VI series of fission product release tests of high-burnup, commercial LWR fuel under severe accident conditions at ORNL. Six similar tests were conducted in a simpler furnace at lower temperatures in the previous HI series. Other ORNL reports describing the work conducted for this project are listed below.

1. M. F. Osborne, R. A. Lorenz, J. R. Travis, and C. S. Webster, "Data Summary Report for Fission Product Release Test HI-1," NUREG/CR-2928 (ORNL/TM-8500), December 1982.

2. M. F. Osborne, R. A. Lorenz, J. R. Travis, C. S. Webster, and K. S. Norwood, "Data Summary Report for Fission Product Release Test HI-2," NUREG/CR-3171 (ORNL/TM-8667), April 1984.

3. M. F. Osborne, R. A. Lorenz, K. S. Norwood, J. R. Travis, and C. S Webster, "Data Summary Report for Fission Product Release Test HI-3," NUREG/CR-3335 (ORNL/TM-8793), April 1984.

4. M. F. Osborne, J. L. Collins, R. A. Lorenz, K. S. Norwood, J. R. Travis, and C. S. Webster, "Data Summary Report for Fission Product Release Test HI-4," NUREG/CR-3600 (ORNL/ TM-9001), June 1984.

5. M. F. Osborne, J. L. Collins, R. A. Lorenz, K. S. Norwood, J. R. Travis, and C. S. Webster, "Data Summary Report for Fission Product Release Test HI-5," NUREG/CR-4037 (ORNL/ TM-9437), May 1985.

6. M. F. Osborne, J. L. Collins, R. A. Lorenz, K. S. Norwood, J. R. Travis, and C. S. Webster, "Data Summary Report for Fission Product Release Test HI-6," NUREG/CR-4043 (ORNL/ TM-9943), September 1985.

7. M. F. Osborne, J. L. Collins, R. A. Lorenz, J. R. Travis, and C. S. Webster, "Design, Construction, and Testing of a 2000°C Furnace and Fission Product Collection System," NUREG/ CR-3715 (ORNL/TM-9135), September 1984.

8. J. L. Collins, M. F. Osborne, R. A. Lorenz, K. S. Norwood, J. R. Travis, and C. S. Webster, "Observed Behavior of Cesium, Iodine, and Tellurium in the ORNL Fission Product Release Program," NUREG/CR-3930 (ORNL/TM-9316), February 1985.

9. K. S. Norwood, "An Assessment of Thermal Gradient Tube Results from the HI Series of Fission Product Release Tests," NUREG/CR-4105 (ORNL/TM-9506), March 1985.

10. M. F. Osborne, J. L. Collins, P. A. Haas, R. A. Lorenz, J. R. Travis, and C. S. Webster, "Design and Final Safety Analysis Report for Vertical Furnace Fission Product Release Apparatus in Hot Cell B, Building 4501," NUREG/CR-4332 (ORNL/TM-9720), March 1986.

11. M. F. Osborne, J. L. Collins, and R. A. Lorenz, "Highlights Report for Fission Product Release Tests of Simulated LWR Fuel," ORNL/NRC/LTR-85/1, February 1985.

12. Toshiyuki Yamashita, "Steam Oxidation of Zircaloy Cladding in the ORNL Fission Product Release Tests," NUREG/CR-4777 (ORNL/TM-10272), March 1988.

13. S. K. Wisbey, "Preliminary Studies of the Morphology of Thermal Gradient Tube Deposits for Fission Product Release Experiments," NUREG/CR-4778 (ORNL/TM-10273), March 1988.

14. C. S. Webster and M. F. Osborne, "The Use of Fiber Optics for Remote Temperature Measurement in Fission Product Release Tests," NUREG/CR-4721 (ORNL/TM-10366), April 1989.

15. M. F. Osborne, J. L. Collins, R. A. Lorenz, J. R. Travis, C. S. Webster, and T. Yamashita, "Data Summary Report for Fission Product Release Test VI-1," NUREG/CR-5339 (ORNL/ TM-11104), June 1989.

16. M. F. Osborne, J. L. Collins, R. A. Lorenz, J. R. Travis, and C. S. Webster, "Data Summary Report for Fission Product Release Test VI-2," NUREG/CR-5340 (ORNL/TM-11105), September 1989.

17. M. F. Osborne, J. L. Collins, R. A. Lorenz, J. R. Travis, C. S. Webster, H. K. Lee, T. Nakamura, and Y.-C. Tong, "Data Summary Report for Fission Product Release Test VI-3," NUREG/CR-5480 (ORNL/TM-11399), April 1990.

18. M. F. Osborne, R. A. Lorenz, J. L. Collins, J. R. Travis, C. S. Webster, and T. Nakamura, "Data Summary Report for Fission Product Release Test VI-4," NUREG/CR-5481 (ORNL/TM-11400), October 1990.

19. M. F. Osborne, R. A. Lorenz, J. R. Travis, C. S. Webster, and J. L. Collins, "Data Summary Report for Fission Product Release Test VI-5," NUREG/CR-5666 (ORNL/TM-11743), October 1991.

20. M. F. Osborne, R. A. Lorenz, J. R. Travis, C. S. Webster, and J. L. Collins, "Data Summary Report for Fission Product Release Test VI-6," NUREG/CR-6077 (ORNL/TM-12416), March 1994.

21. M. F. Osborne, R. A. Lorenz, J. R. Travis, "Preliminary Results from ORNL Fission Product Release Test VI-7," ORNL/NRC/LTR-94/2, February 1994.

22. R. A. Lorenz and M. F. Osborne, "A Summary of ORNL Fission Product Release Tests with Recommended Release Rates and Diffusion Coefficients," NUREG/CR-6261 (ORNL/TM-12801) to be published.

# 1 Introduction

This report summarizes data from the seventh high-temperature test in a vertical test apparatus. This series of tests was designed to investigate fission product release from light-water-reactor (LWR) fuel as functions of temperature (in the range of 2000 to 2700 K) and atmosphere (steam, air, and/or hydrogen) at atmospheric pressure. Six tests in an earlier series, denoted HI-1 through HI-6, were conducted in a horizontal furnace under similar conditions—temperatures of 1675 to 2275 K (1400 to 2000°C) in steam atmospheres. The HI series tests were analyzed and reported previously,[1] and comparable data summary reports are listed as items 1 through 6 in the Foreword. After revising the test apparatus to accommodate the vertical furnace, a new series of tests to higher temperatures, denoted VI-1 through VI-7, was initiated.[2-7] All of this work has been summarized in *Nuclear Safety*.[8]

The purpose of this project, which is sponsored by the U.S. Nuclear Regulatory Commission (NRC), is to obtain the experimental data needed to reliably assess the consequences of a variety of heatup accidents in LWRs.[9] The specific objectives were

1. to obtain fission product release and behavior data applicable to the analysis of reactor accidents and

2. to apply these data to the development of fission product release and transport models.

Tests of high-burnup LWR fuel were emphasized throughout this project. However, the applicability of simulated fuel (unirradiated $UO_2$ containing radioactive fission product tracers) was considered, and several simulant tests were conducted to provide valuable data about the behavior of specific fission product species[10] and to allow comparison of results with other experimental work.[11] All tests have been conducted at atmospheric pressure in helium mixed with a reactive gas (steam, air, and/or hydrogen) in a hot cell–mounted test apparatus.[12]

The procedures and techniques used in preparing and conducting Test VI-7, as well as in posttest examination and analysis, were very similar to those used in earlier tests. The analytical techniques employed are listed in Table 1.1. This report provides a brief description of this test and a compilation of all available results. Thorough data evaluation and correlation of all results through Test VI-6 are included in a recent comprehensive review.[13] .

## Table 1.1. Analytical techniques used for fission product analysis

| Technique | Time | Location | Elements |
|---|---|---|---|
| Gamma spectrometry | Pretest, posttest | Fuel specimen | Long-lived, gamma-emitting fission products — Ru, Sb, Cs, Ce, Eu |
| | On-line | Thermal gradient tube (TGT), charcoal traps, filters | Cs, Kr |
| | Posttest | Furnace components, TGT, filters | Ru, Sb, Cs, Ce, Eu |
| Neutron activation analysis | Posttest | Charcoal; solutions from furnace, TGT, filters | I, Br |
| Chemical analysis | Posttest | Furnace, filters | U, Pu |
| Inductively coupled plasma-emission spectrometry | Posttest | Acid solutions from furnace, TGT, or filters | Many cations, especially Sr, Mo, Ru, Te, Ba, U |

2

# 2 Test Description

The vertical test apparatus[12] is operated remotely and is capable of conducting tests at temperatures up to 2700 K for time periods up to 60 min in reactive atmospheres, such as steam, air, and/or hydrogen mixed with helium. Details of the furnace are shown in Figure 2.1, and the entire test apparatus installed in the hot cell is illustrated in Figure 2.2. Both manual and automatic optical pyrometers are used for temperature measurement, supplemented by thermocouples during the low-temperature heatup phase. Temperature control is accomplished by manual operation of the radiofrequency power supply.

The released fission products are collected in three sequentially operated, parallel collection trains. Each train is composed of (1) a 7.6-mm-ID platinum or stainless steel-lined thermal gradient tube (TGT) designed for vapor condensation, (2) a filter package containing graduated fiberglass filters for aerosol collection and heated charcoal that had been impregnated with Triethylenediamine (TEDA) for iodine sorption, and (3) cold charcoal traps for rare gas collection. The on-line releases of $^{85}$Kr and $^{137}$Cs are monitored by NaI(Tl) detectors observing these collector components (see Figure 2.2). In steam atmosphere tests, a hot CuO bed is used to oxidize the hydrogen generated by reaction of steam with the Zircaloy cladding. The collection of this water in a condenser is measured continuously by a modified conductivity meter, thereby indicating the oxidation rate of the cladding. Details of the fission product collection system are shown in Figure 2.3. Included in the Test VI-7 apparatus were three radiation detectors that were collimated to monitor the radioactivity (especially $^{134}$Cs, $^{137}$Cs, and $^{154}$Eu) in the top, middle, and bottom regions of the fuel specimen. Data from these instruments should indicate any movement or collapse of the fuel during the test.

The tests conducted in this vertical apparatus assumed that temperature (2000 to 2700 K) was the dominant variable. The flow rates of reactive gas ($\sim 1.0$ L/min) and time at high temperature ($\sim 60$ min) were considered to be important but secondary variables. The objectives of this particular test were to obtain release rate data from the Monticello boiling water reactor (BWR) fuel heated at 2000 and 2300 K in moist air to effect oxidation of the Zircaloy cladding, and perhaps of the UO$_2$ fuel. Test VI-1 in which a specimen of Oconee fuel

of the same burnup was heated under the same time and temperature conditions in steam (no air) provided a basis for comparing atmospheric effects.

## 2.1 Fuel Specimen Data

The fuel specimen used in this test was cut from fuel rod G5 of bundle BND-0304, which had been irradiated in the Monticello BWR from May 1974 to February 1980, attaining a burnup of 40.3 MWd/kg U as part of an extended burnup program. The available fabrication and irradiation data are summarized in Table 2.1, and postirradiation examination of this fuel was described by Pasupathi et al.[14] Fission product inventories for the specimen were measured by direct gamma spectrometry of the fuel (for the long-lived gamma-emitting species only) and were calculated with the ORIGEN2 computer program,[15] as shown in Tables 2.2 and 2.3. Since a specimen from the same Monticello fuel rod was heated to about the same temperature in Test HI-6, comparison of Tests VI-7 and HI-6 results will be appropriate.

Fission gas release data and gamma scans for the entire rod before it was sectioned were reported by Pasupathi et al.[14] These data indicated that the rod had experienced no unusual temperature, power, or burnup histories during irradiation. Therefore, we assumed that no unusual fission product migration and/or reactions had occurred. Based on the available information, we estimate that $\sim 2\%$ of the total krypton generated in the fuel specimen had been released during irradiation.

In preparation for use in Test VI-7, tapered end caps of Zircaloy-2 were pressed onto the ends of the 15-cm-long fuel specimen. These end caps were not expected to provide gas seals, but rather to prevent loss of the fractured UO$_2$ fuel during subsequent handling. Because the original bottom end cap had not included the pin to facilitate vertical mounting, a second end cap with a mounting pin was pressed onto the original end cap prior to Test VI-7. A small hole, 1.6 mm in diameter, was drilled through the cladding at midlength to serve as a standard leak for gas release during the heatup phase of the test. These details are shown in Figure 2.4.

The axial distributions of several fission products in the fuel specimen, as determined by gamma-ray spectrometry through a 1-cm window at 1-cm intervals, is shown in

3
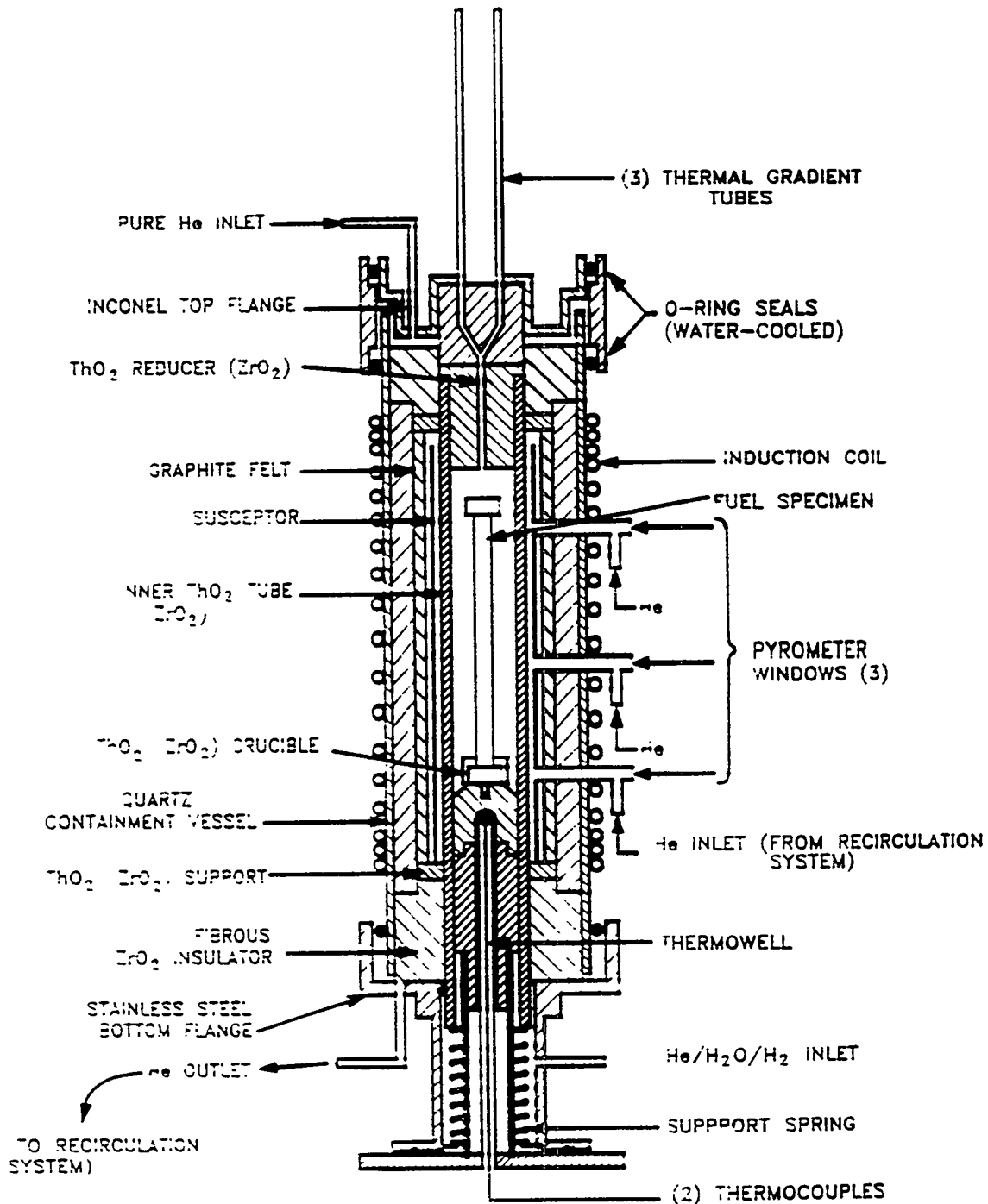
Description

Figure 2.1 Vertical fission product release furnace, as used in Test VI-6

4
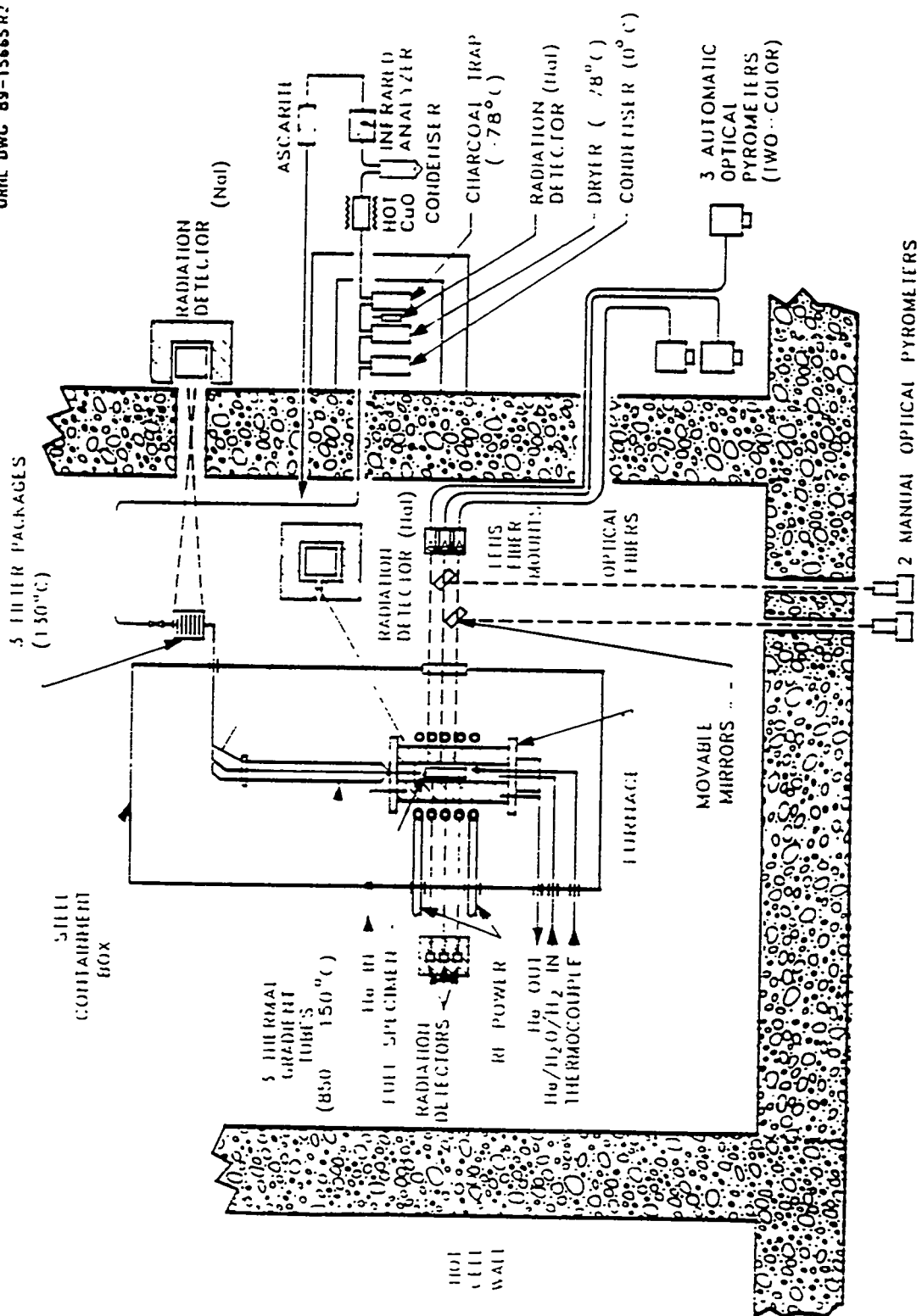
Figure 2.2 Vertical fission product release apparatus

5

Description

ORNL DWG 90-14768
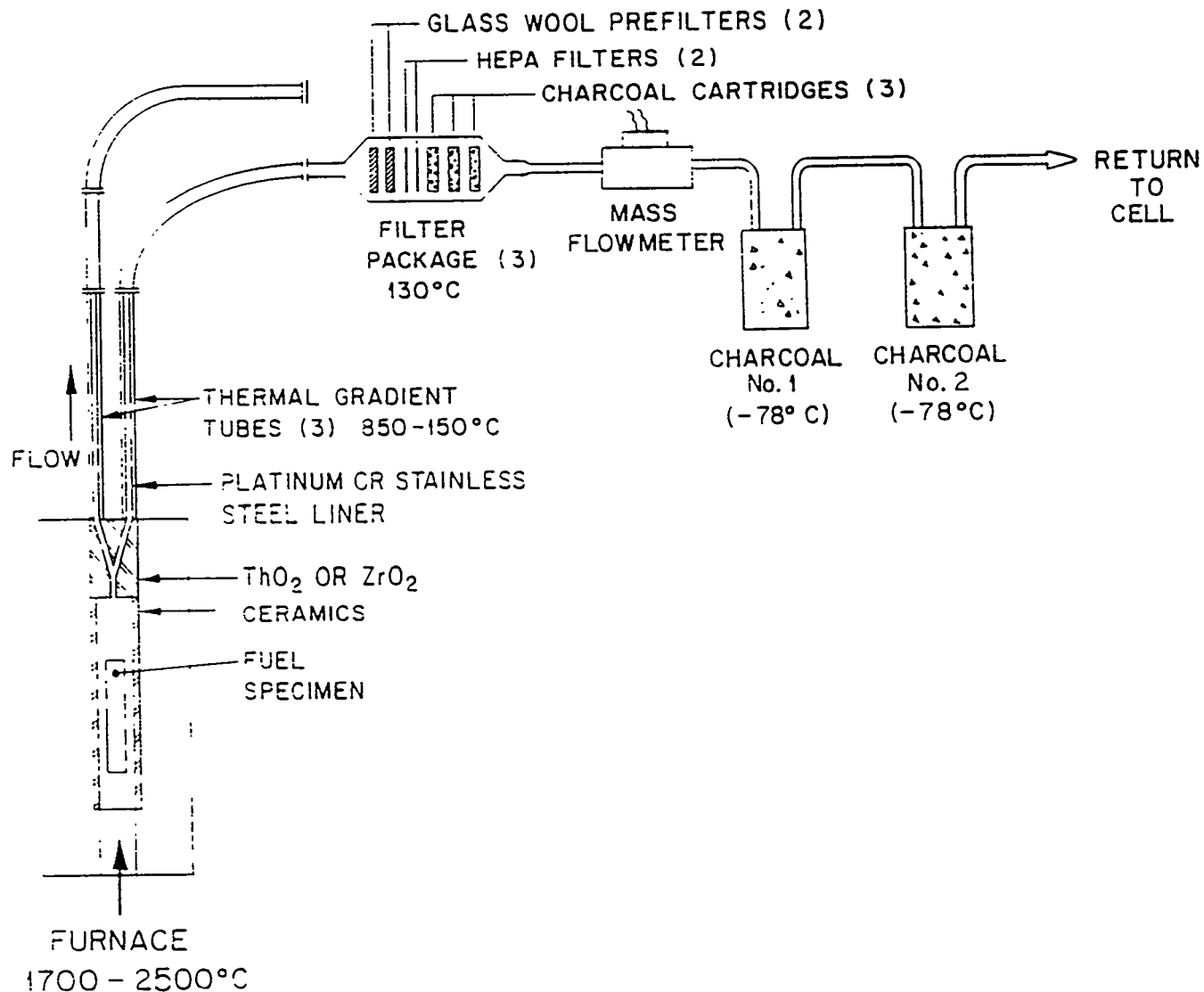


Figure 2.3  Components of the fission product collection system

Table 2.1 Data for fuel specimen used in Test VI-7

| | |
|---|---|
| **Fuel rod identification** | BND-0304 (G-5)<br>Section 3 |
| **Bundle type** | GE, 8 × 8 |
| **Irradiation data** | |
| Period | May 1974 to February 1980 |
| Average burnup of rod | ~31.4 MWd/kg |
| Burnup of test specimen | ~40.3 MWd/kg |
| **Fuel rod characteristics (unirradiated)** | |
| Zircaloy-4 cladding | 1.243-cm (0.489-in.) OD<br>1.072-cm (0.422-in.) ID |
| Initial enrichment | 2.87% $^{235}$U |
| Initial helium fill | Atmospheric pressure |
| **Test specimen characteristics** | |
| Length | 15.2 cm (6.0 in.) |
| Specimen fuel loading | 126.0 g $UO_2$ (112.3 g U) |
| Weight of Zircaloy cladding and end caps | 52.5 |
| Total weight of specimen | 178.5 |
| Gas release during irradiation | 1.6% (from whole rod)<br>2% (from specimen) |

Description

**Table 2.2  Test VI-7 fuel fission product inventories
(calculated using ORIGEN2 on 8/14/84)**

| Element | Monticello fuel rod<br>(g/MTIHM, 7/15/81) | VI-7 specimen[*]<br>(g at 7/94) |
|---------|---------|---------|
| Kr | 4.126E+02 | 4.63E−02 |
| Rb | 3.874E+02 | 4.35E−02 |
| Sr | 9.450E+02 | 1.06E−01 |
| Y | 5.085E+02 | 5.71E−02 |
| Zr | 4.108E+03 | 4.61E−01 |
| Mo | 4.039E+03 | 4.54E−01 |
| Ru | 2.857E+03 | 3.21E−01 |
| Sb | 3.027E+01 | 3.40E−03 |
| Te | 5.985E+02 | 6.72E−02 |
| I[**] | 2.389E+02 | 2.68E−02 |
| Xe | 6.354E+03 | 7.14E−01 |
| Cs | 3.302E+03 | 3.71E−01 |
| Ba | 1.868+03 | 2.10E−01 |
| Ce | 2.891E+03 | 3.25E−01 |
| Eu | 2.055E+02 | 2.31E−02 |
| Total FP | 4.147E+04 | 4.66E+00 |
| U | 9.476E+05 | 1.06E+02 |
| Pu | 1.000E+04 | 1.12E+00 |

[*]Initial loading in Test VI-7 fuel specimen was 112.3 g U or 1.123E-4 MTIHM.
[**]I values corrected:  ORIGEN2 × 0.82.

Table 2.3 Test VI-7 fuel inventories and radioactivities
(Monticello fuel, from ORIGEN2 calculation of 8/14/84)

| Nuclide | ORIGEN2 at 7/15/81 Monticello fuel | | Test VI-7 specimen[*] | |
|---|---|---|---|---|
| | (Ci/MTIHM) | (g/MTIHM) | (Ci at 7/94) | (g at 7/94) |
| $^{60}$Co | 3.933E+02 | 3.477E−01 | 7.995E−03 | 3.905E−05 |
| $^{85}$Kr | 8.744E+03 | 2.228E+01 | 4.238E−01 | 2.502E−03 |
| $^{90}$Sr | 7.553E+04 | 7.535E+00 | 6.217E+00 | 8.462E−04 |
| $^{106}$Ru | 1.829E+05 | 5.464E+01 | 2.688E−03 | 6.136E−03 |
| $^{125}$Sb | 9.482E+03 | 9.108E+00 | 4.122E−02 | 1.031E−03 |
| $^{129}$I | 3.214E−02 | 1.820E+02 | 3.609E−06 | 2.044E−02 |
| $^{134}$Cs | 1.158E+05 | 8.950E+01 | 1.641E−01 | 1.005E−02 |
| $^{137}$Cs | 1.189E+05 | 1.336E+03 | 9.906E+00 | 1.534E−01 |
| $^{144}$Ce | 1.875E+05 | 5.875E+01 | 1.958E−04 | 6.598E−03 |
| $^{154}$Eu | 1.376E+04 | 5.096E+01 | 5.552E−01 | 5.723E−03 |
| Total FP | 1.367E+06 | 4.147E+04 | 1.732E+01 | 4.657E+00 |
| $^{235}$U | 8.486E−03 | 3.924E+03 | 9.530E−07 | 4.407E−01 |
| $^{238}$U | 3.160E−01 | 9.397E+05 | 3.549E−05 | 1.055E+02 |
| Total U | 5.003E+00 | 9.476E+05 | 3.644E−05 | 1.064E+02 |
| $^{238}$Pu | 4.559E+03 | 2.662E+02 | 4.620E−01 | 2.989E−02 |
| $^{239}$Pu | 3.083E+02 | 4.958E+03 | 3.461E−02 | 5.568E−01 |
| $^{240}$Pu | 5.878E+02 | 2.578E+03 | 6.592E−02 | 2.895E−01 |
| $^{241}$Pu | 1.455E+05 | 1.412E+03[*] | 8.854E+00 | 1.586E−01 |
| $^{242}$Pu | 3.018E+00 | 7.903E+02 | 3.389E−04 | 8.874E−02 |
| Total Pu | 1.509E+05 | 1.000E+04 | 9.417E+00 | 1.123E+00 |

[*]Initial loading in Test VI-7 fuel specimen was 112.3 g U. or 1.123 E-4 MTIHM.
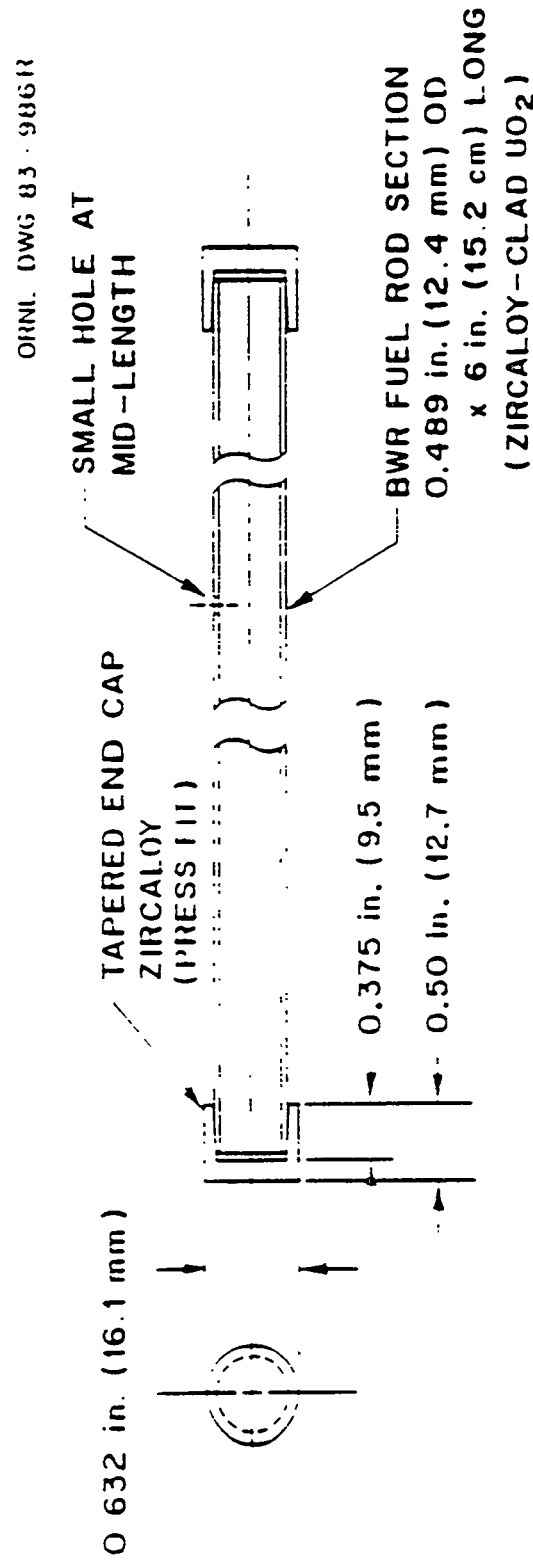
Figure 2.4   Dimensions of fuel specimen used in Test VI-7

Figure 2.5. This profile indicates uniform burnup of the fuel and fission product content along the specimen.

## 2.2 Test Conditions and Operation

As in each of the previous experiments, the test apparatus was assembled by direct handling, which is possible because the hot cell and test apparatus are decontaminated after each test. Also, new $ZrO_2$ furnace components, new TGT liners of 0.003-in. (0.076-mm)-thick platinum, and new filter package components were prepared and installed. In most previous tests, platinum TGT liners have been used to provide a relatively unreactive surface for the deposition of fission products, so that effects on the chemical forms of the deposits would be minimized. In some cases, however, stainless steel liners have been used to simulate the effects of realistic reactor material on the deposits. Only the transfer and loading of the highly radioactive fuel specimen and the final closure of the furnace and containment box were done remotely, and no in-cell operations were required during the test. Before heating was begun, the test apparatus was evacuated and purged with helium.

This test was intended to investigate the effects of oxidation by moist air on fission product release at 2300 K. In earlier tests in steam, the oxidized cladding had remained largely intact, serving as a barrier to effective $UO_2$-steam contact, but no air had been included in previous high temperature tests. The operating conditions are summarized in Table 2.4, and the temperature history is shown in Figure 2.6. The heatup rate in Test VI-7 was ~25 K/min, and the cooldown rate (after the high temperature period) was ~33 K/min.

The more important events during the test are listed in the test chronology (Table 2.5). The time periods for operation of the three collection trains (see Figure 2.6) were 0 to 85 min for Train A; 85 to 95 min for Train B; and 95 min to the end of the test, ~211 min, including cooldown for Train C. A preheat period was included to slowly heat the specimen to ~550 K in helium prior to beginning

airflow to the furnace. Time zero was defined as that time when the controlled heating ramp was begun, with stable gas (moist air + helium) flow through the warm furnace established. Temperature measurement and control were generally good. The 6-min period at ~1425 K was included to compare the data from the optical pyrometers, thereby ensuring accurate temperature measurement and control, and to allow additional time for heatup of ceramics in the outlet end of the furnace before any significant release of fission cooldown for Train C. A preheat period was included to slowly heat the specimen to ~550 K in helium prior to beginning airflow to the furnace. Time zero was defined as that time when the controlled heating ramp was begun, with stable gas (moist air + helium) flow through the warm furnace established. Temperature measurement products had occurred. As indicated in Figure 2.6, the planned time/temperature conditions were accomplished.

The planned atmosphere for Test VI-7 was a mixture of 1-L/min air and 0.5-L/min helium saturated with water vapor at 323 K (50°C). The initial water saturation temperature during test Phase A was set at 303 K (30°C), to limit the cladding oxidation rate and keep the H2/O2 ratio below the ignition limit. Then, when a large fraction of the Zircaloy cladding had been oxidized at a fuel temperature of 2000 K, the water saturation temperature was quickly increased to 323 K (50°C) for the remainder of the test, as indicated in Table 2.4. The gas flow history for the entire test period is illustrated in Figure 2.7.

As in previous tests, a small amount of krypton release was observed early in the heating cycle (at ~600 to 700 K). This krypton is believed to be gas released from the fuel during irradiation and adsorbed on fuel and cladding surfaces until its desorption during the test heatup. As indicated in Figure 2.8, significant krypton release as a result of diffusion from the $UO_2$ began at ~1630 K (1357°C). A trace of cesium was detected on the TGT at a slightly lower temperature, ~1500 K (1227°C). While the release of krypton appeared to cease at the end of the 2300 K (Phase C) test period, cesium collection on both TGT C and filter C continued for ~10 min as the fuel cooled.

Description
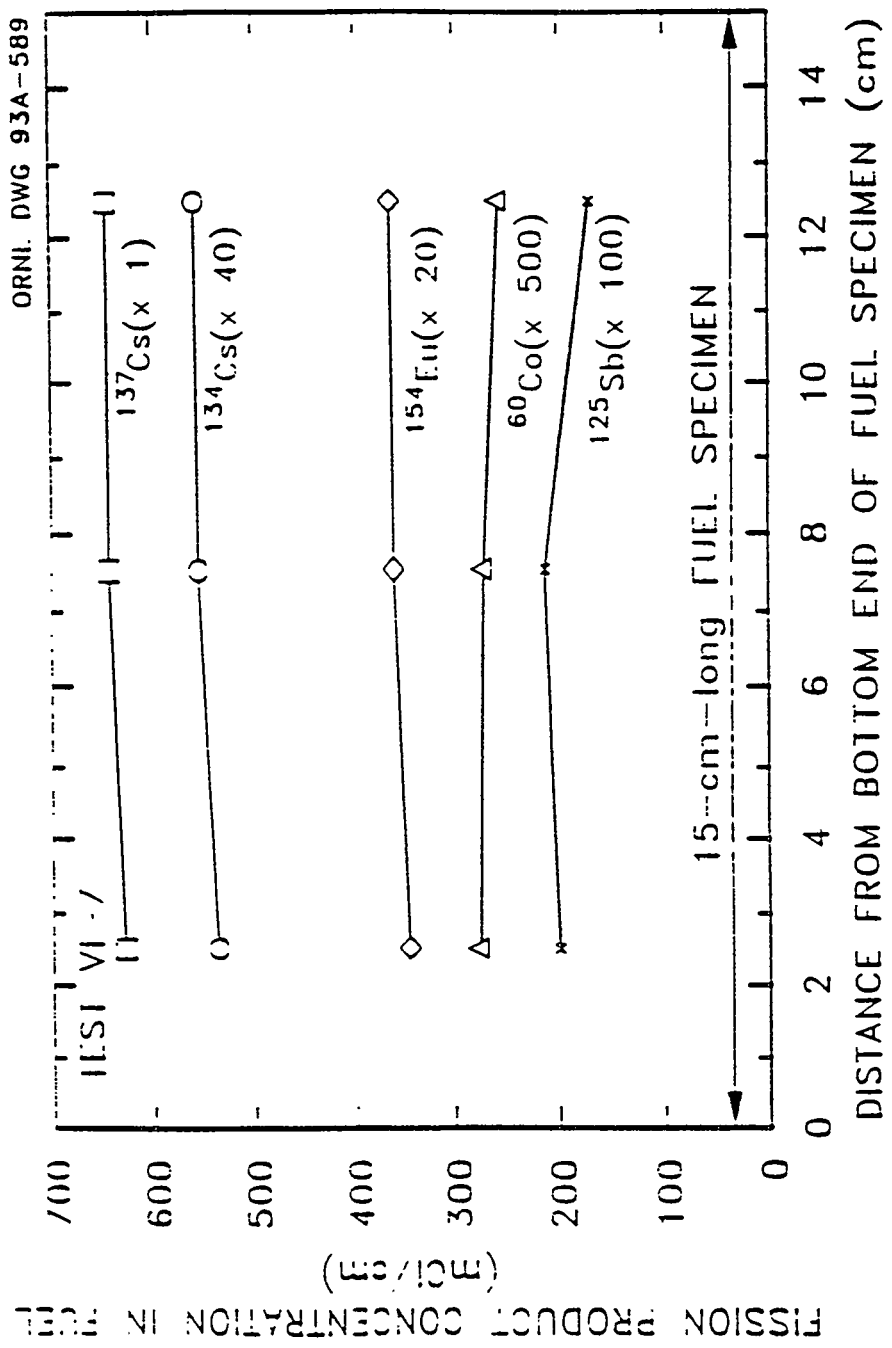


Figure 2.5  Axial distribution of $^{134}$Cs, $^{137}$Cs, $^{125}$Sb, $^{154}$Eu, and $^{60}$Co in Test VI-7 fuel specimen

Table 2.4 Operating data for Test VI-7

---

**Specimen temperature**

| | |
|---|---|
| At start of heatup ramp, K | ~500 |
| During first plateau to check pyrometers, K | 1430 |
| Phase A heatup rate to 2000 K, K/min | 23 |
| During 20-min Phase A plateau, average, K | 2025 |
| Phase B heatup rate to 2300 K, K/min | 26 |
| During 20-min Phase C plateau, average, K | 2307 |
| Cooldown rate, K/min | 33 |
| Time above 2000 K, min | 57 |

**Nominal gas flow rate (L/min at 20°C and 1 bar)[a]**

| | |
|---|---|
| During Phase A heatup to 2000 K: | |
|     Air to fuel specimen, saturated with water at 30°C | 1.8 |
|     Helium to susceptor (and fuel specimen) | 0.4 |
|     Helium to thermowell (and fuel specimen) | 0.1 |
|     Recirculation/purification system | 1.5 |
| | |
| During 2000 and 2300 K test period: | |
|     Air to fuel specimen, saturated with water at 50°C | 1.0 |
|     Helium to susceptor (and fuel specimen) | 0.4 |
|     Helium to thermowell (and fuel specimen) | 0.1 |
|     Recirculation/purification system | 1.5 |

---

[a]Measured by mass flowmeters. Absolute pressure in furnace was 0.09925 MPa (744.4 mm Hg).

Description
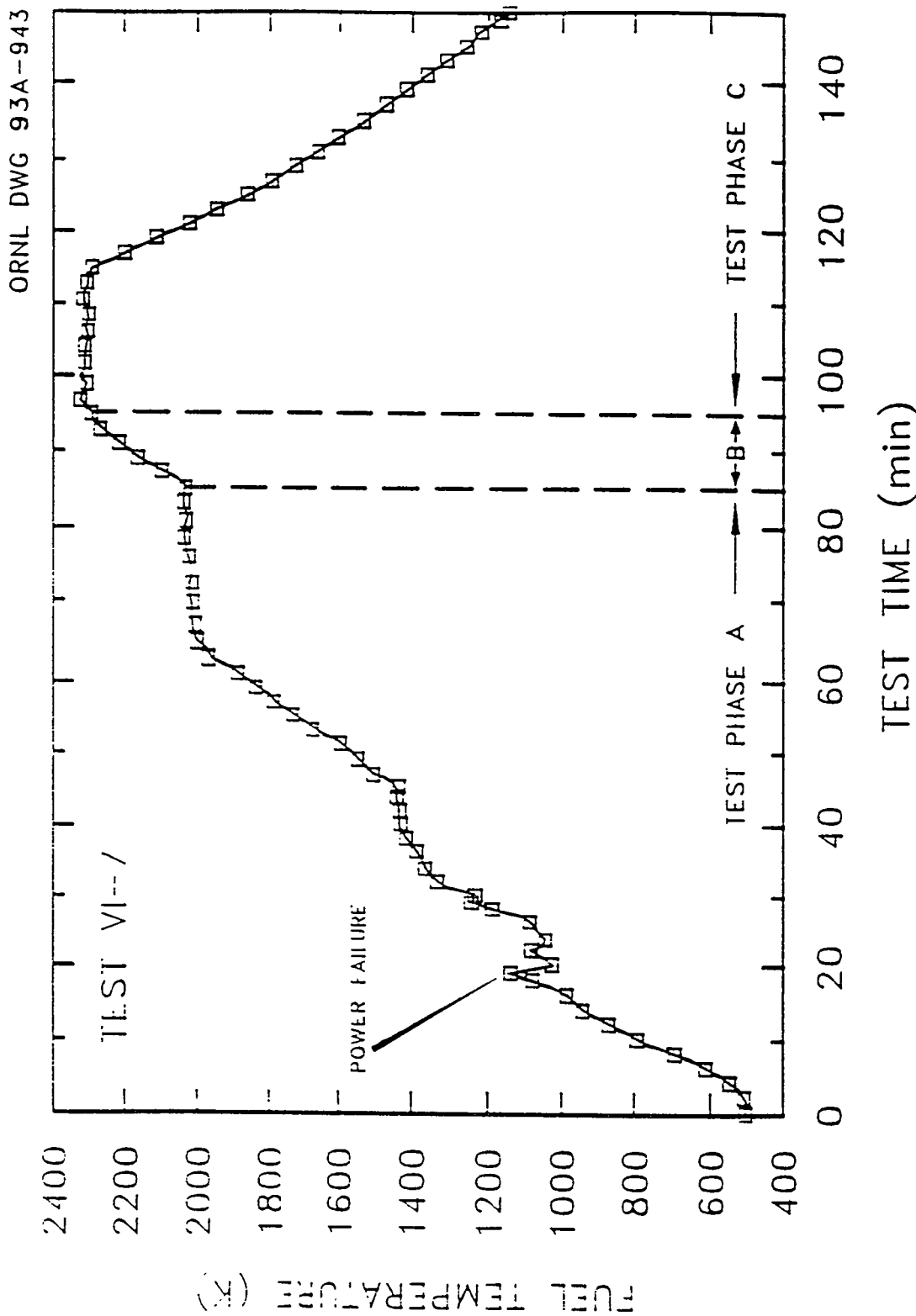


Figure 2.6 Temperature history of Test VI-7 showing Test Phases A, B, and C

14

Table 2.5 Chronology of Test VI-7, conducted September 16, 1993.
Fuel specimen loaded into furnace September 15, 1993

| Event/observation | Clock (h) | Time (min) | Temperature at test midpoint of fuel (K, corrected) |
|---|---|---|---|
| Vacuum and pressure tests | 930 | | |
| Complete alarm checks | 1000 | | |
| Begin system preheat | 1120 | | RT * |
| Begin furnace preheat, with gas flow to furnace | 1130 | | RT * |
| Stable flow and temperature | 1230 | | 480 ** |
| **Test Phase A** | | | |
| Start ramp to ~1600 K, at ~30 K/min | 1300 | 0 | 470 ** |
| Heatup based on thermocouple | 1320 | 20 | 960 ** |
| Begin accurate pyrometer measurement | 1335 | 35 | 1305 |
| Reached stable plateau | 1339 | 39 | 1424 |
| Resume ramp to 2000 K | 1345 | 45 | 1434 |
| Krypton release observed | 1352 | 52 | 1634 |
| Cesium detected on TGT | 1358 | 58 | 1804 |
| Reached 2000 K plateau. increase steam generator to 50°C | 1405 | 65 | 2000 |
| After 20 min at 2000 K, end Phase A | 1425 | 85 | 2033 |
| **Test Phase B** | | | |
| Begin Phase B. heat to 2300 K at ~30 K/min | 1425 | 85 | 2033 |
| End Phase B. at 2300 K | 1435 | 95 | 2292 |
| **Test Phase C** | | | |
| Begin Phase C. 20 min at 2300 K | 1435 | 95 | 2292 |
| Rapid cesium deposition on filters | 1437 | 97 | 2322 |
| End 2300 K plateau. reduce power to cool at ~50 K/min | 1455 | 115 | 2292 |
| Power off | 1509 | 129 | 1724 |
| Cooling at ~30 K/min | 1520 | 140 | 1385 |
| Air flow ended. helium continued | 1527 | 147 | 1214 |
| Last pyrometer measurements | 1530 | 150 | 1146 |
| End Phase C. helium flow reduced | 1631 | 211 | ~500 |

*RT = room temperature.
**Based on thermocouple measurement.

Description
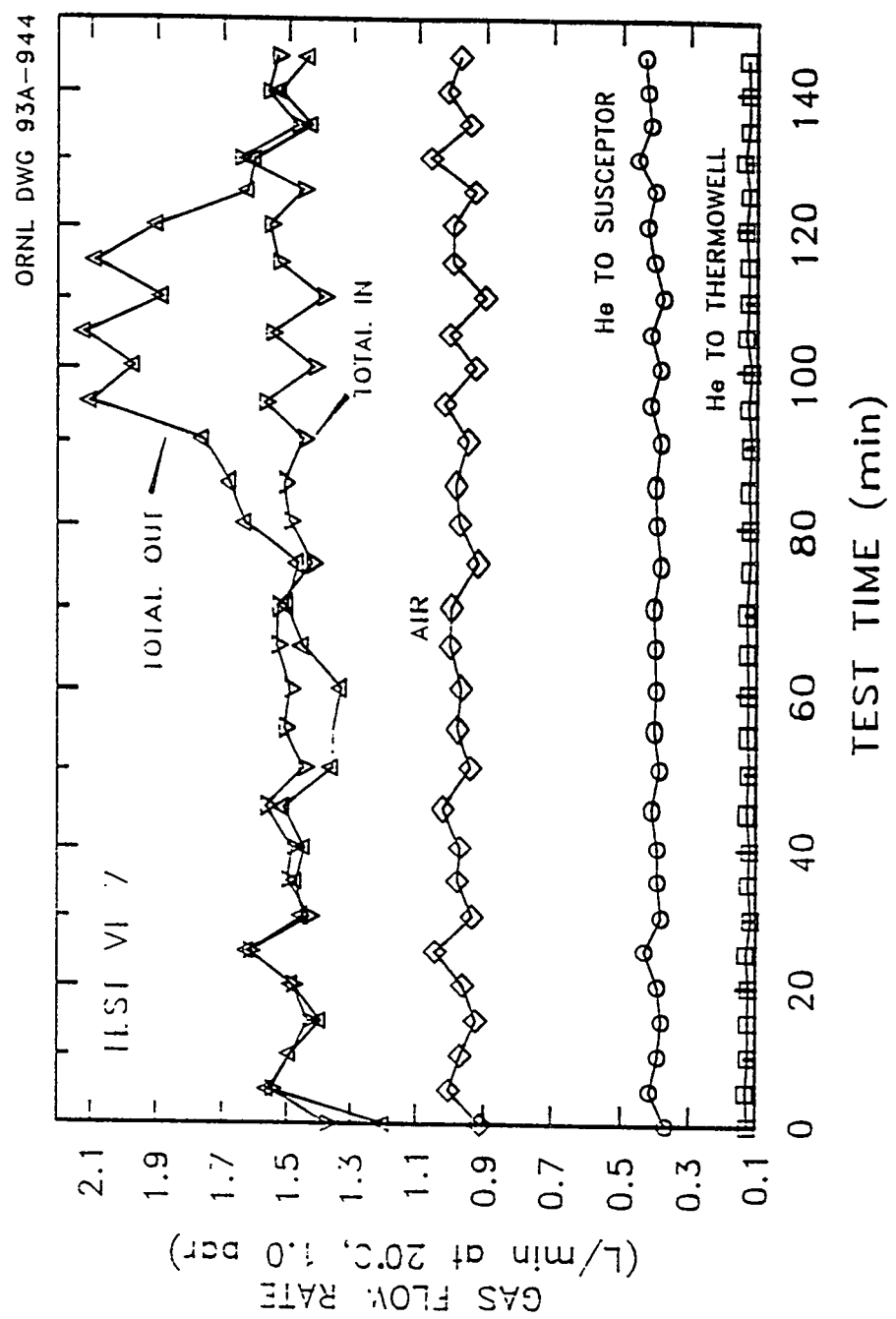


**Figure 2.7  Gas flow history in Test VI-7**
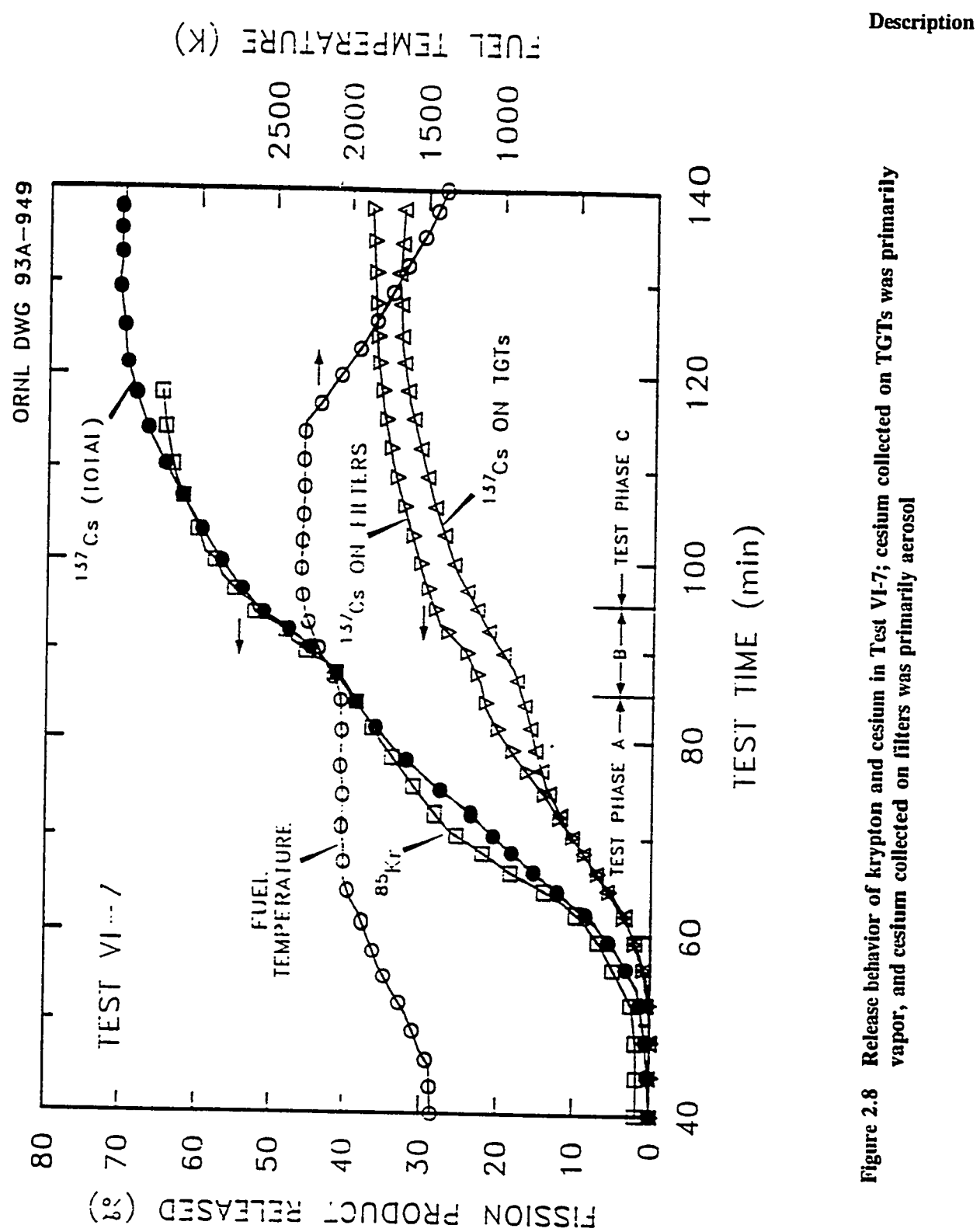
Figure 2.8 Release behavior of krypton and cesium in Test VI-7; cesium collected on TGTs was primarily vapor, and cesium collected on filters was primarily aerosol

17

## 2.3 Posttest Disassembly and Examination

Before disassembly was begun, the apparatus was monitored with an in-cell ion chamber for the distribution of radioactivity. The highest concentrations of radioactivity were found at the furnace exit (190 rem/h) and at about midlength of the TGTs (200 rem/h). Higher levels of radioactivity along the TGTs than on the filters (~60 rem/h) and the furnace (~150 rem/h) were at least partially a result of additional shielding and the distance from the source for the filters and furnace. These distributions and levels of radioactivity were similar to those found after previous VI tests at 2300 K.

Initially, the filter assemblies and the furnace top flange-TGT assembly, containing the TGT liners, were removed, sealed, and transferred to another hot cell to avoid potential cross contamination from other components. The ZrO$_2$ top end plug was removed from the furnace tube to allow observation of the interior, showing that the fuel specimen appeared to be in its initial upright position. After inspection, the furnace cavity was filled with epoxy resin to preserve the geometry of the degraded fuel specimen during handling, gamma spectrometry, sectioning, or any other operations. After removal of the fuel-furnace tube assembly from the furnace, it was analyzed in detail by gamma spectrometry then cut into short sections for visual examination. Two of these radial sections — one from near the bottom (inlet) end of the specimen and one from near the top (outlet) end — were selected for metallographic examination to investigate the extent of cladding oxidation and changes in fuel microstructure.

# 3 Test Results

## 3.1 Gamma Spectrometry Data

After the test, all experimental components and collectors were analyzed under well-defined geometry for quantitative analysis of the gamma-emitting fission products. In order to determine the effective shielding to obtain a mass balance for cesium, the previously proven empirical method for adjusting the self-shielding factor for several of the principal $^{134}$Cs gamma-ray energies was used.[2] This technique provides good results for all of the long-lived, gamma-emitting nuclides.

Pretest gamma spectrometric analysis of the 15.2-cm-long fuel specimen was used to determine the fission product inventories of $^{106}$Ru, $^{125}$Sb, $^{134}$Cs, $^{137}$Cs, and $^{154}$Eu in the fuel and $^{60}$Co in the cladding. As noted previously in Section 2, a calculation by the computer program ORIGEN2 supplied the inventory values for all fission products, activation products, and fuel nuclides; these are shown in Tables 2.2 and 2.3. Based on posttest measurements at 1-cm intervals along the fuel specimen, as shown in Figure 3.1, the axial concentrations of cesium and antimony were lowest at the bottom (gas inlet) end, and increased with distance toward the top (gas outlet) end, indicating higher releases at the bottom end. Such a release gradient, which had not been observed in any previous test, could be the result of either a temperature gradient (higher release at higher temperature) or an oxidation gradient (higher release with fuel oxidation) along the specimen. Neither experience nor operational data revealed any evidence of a temperature gradient, but calculations indicated that an oxidation gradient was likely. Whereas the lower end of the specimen was always exposed to excess oxygen and steam, rapid reactions with the Zircaloy cladding reduced the concentrations of these oxidants and produced hydrogen in place of steam so that the atmosphere over the upper end of the specimen was reducing for almost half of the test period. Furthermore, radial sections of fuel that were selected for metallographic examination showed some differences in the appearance of the oxidized cladding. The results of these examinations will be discussed in Section 3.7. In addition to the fission products, the axial distribution of the $^{60}$Co in the Zircaloy cladding, also shown in Figure 3.1, indicates higher release at the bottom end.

In general, we believe that $^{144}$Ce is the best indicator of fuel location in gamma scans. Because of the long decay time for the fuel in Test VI-7 (~13 y), however, the counting precision for $^{144}$Ce ($T_{1/2}$ = 284 d) was poor. Therefore, $^{154}$Eu, which experienced high release under the reducing conditions in Tests VI-4 and VI-5 but only very low release (<1%) in oxidizing environments, is considered to be the best indicator for the location of $UO_2$ fuel in Test VI-7. As seen in Figure 3.1, the axial distribution of $^{154}$Eu remained flat, indicating no significant redistribution of $UO_2$ during the test.

As has been typical of these tests of high-burnup, long-decayed fuel, $^{137}$Cs and $^{134}$Cs were the dominant activities in almost all samples of released material and interfered with the analysis of less abundant fission products. The integral releases of krypton and cesium, as functions of time and temperature, are illustrated in Figure 2.8. These curves show high release rates for both krypton and cesium from the time temperatures reached ~1800 K until cooldown began after completion of the 2300 K period, a total of ~60 min. As observed in all previous tests, the release behaviors of krypton and cesium were quite similar throughout the test.

A summary of the fractional release results for $^{85}$Kr, $^{125}$Sb, $^{137}$Cs, and $^{60}$Co, as determined by gamma spectrometry, is presented in Table 3.1. In addition, data for $^{129}$I, obtained by neutron activation analysis, are shown. Although no data for $^{134}$Cs are shown, the agreement with $^{137}$Cs was consistently good (within ±3%) at all locations. Since there is no apparent reason for a separation of the two cesium radionuclides, this is a good indication of the precision of the analyses.

The distribution of cesium within the test apparatus is shown in detail in Table 3.2. The fraction of the cesium released from the fuel but retained in the furnace, ~7%, was typical of tests in oxidizing atmospheres.[7] Previous studies of cesium deposited on $ZrO_2$ furnace ceramics at high temperature (>1300 K) indicated a reaction to form a cesium compound, probably $Cs_2ZrO_3$.[17] This compound appeared to be stable in the range ~1100 to 1500 K but decomposed at higher temperatures.[18]
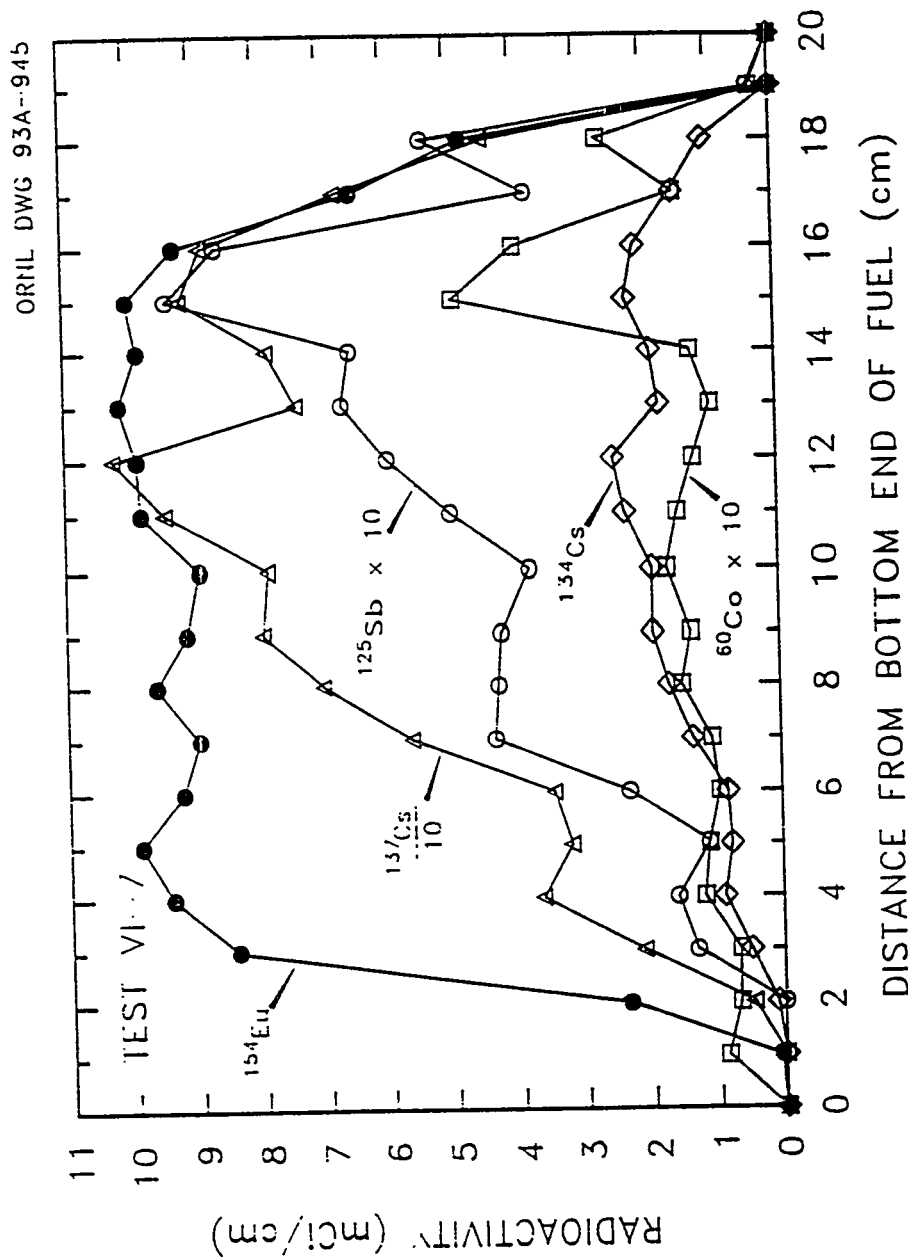
**Figure 3.1** Distribution of radionuclides in fuel specimen after Test VI-7. Note lower concentrations of $^{137}$Cs and $^{125}$Sb near bottom (gas inlet) end of fuel

20

Table 3.1  Summary of fission product release data for Test VI-7

| Component/ collector | Operating time at T>000 K (min) | Percentage of fission product inventory collected during each test phase* | | | | |
|---|---|---|---|---|---|---|
| | | $^{85}$Kr | $^{129}$I | $^{125}$Sb | $^{137}$Cs | $^{60}$Co** |
| Furnace | 57 | 0 | 1.7 | 25.3 | 7.3 | 22.0 |
| Train A | 20 | | | | | |
| TGT | | | | 0 | 15.7 | 0.32 |
| Filters | | | | 0 | 21.0 | 0.65 |
| Total | | 41 | 21.9 | 0 | 36.7 | 0.97 |
| Train B | 10 | | | | | |
| TGT | | | | 0 | 4.2 | 0.50 |
| Filters | | | | 4.8 | 6.4 | 0.93 |
| Total | | 15 | 7.5 | 4.8 | 10.6 | 1.43 |
| Train C | | | | | | |
| TGT | | | | 6.3 | 8.0 | 1.89 |
| Filters | | | | 15.2 | 8.8 | 3.53 |
| Total | | 13 | 10.3 | 21.5 | 16.8 | 5.41 |
| Total for test | 57 | 69 | 41.5 | 51.5 | 71.4 | 29.8 |

*Inventories based on fuel analysis and ORIGEN2 calculations.
**$^{60}$Co is not a fission product, rather an activation product in the cladding.

Table 3.3  Physical forms of cesium released from furnace in Test VI-7

| Collection period | Amount in designated form (% or inventory) | | |
| | Vapor | Aerosol | Total |
|---|---|---|---|
| A | 24.5 | 32.7 | 57.2 |
| B | 6.6 | 10.0 | 16.6 |
| C | 12.5 | 13.8 | 26.3 |
| Total A+B+C | 43.6 | 56.5 | 100 |

The cesium released from the furnace was approximately equally divided between vapor (44%, as indicated by condensation in the thermal gradient tubes) and aerosol (56%, as indicated by collection further downstream, primarily on the filters). These distribution data are shown in Table 3.3. The somewhat higher fraction in aerosol form is consistent with previous data under oxidizing conditions, whereas vapor forms have dominated under reducing (hydrogen atmosphere) conditions.[6]

The measured distributions for the released [125]Sb and ^{60}Co within the test apparatus are shown in Table 3.4. Although [125]Sb is of relatively low yield and is not among the most hazardous fission products, it has an intermediate-length half-life and strong gamma rays, which make it easily detected. Furthermore, [125]Sb has been shown to behave much like and to be a good indicator for tellurium, a highly hazardous fission product element that is more difficult to measure because it has no long-lived gamma-emitting isotopes. Like tellurium, we believe antimony is released from the fuel in elemental form but combines (probably as an alloy) with the Zircaloy cladding and is eventually released as the cladding approaches complete oxidation.[9] In addition, similar behavior for tellurium and antimony is indicated in the TGTs, as discussed by Norwood.[20] The much larger amounts of ^{137}Cs compared with [125]Sb at all locations, because the cesium exceeded the antimony inventory in the fuel by more than two orders of magnitude, indicate the difficulty in measuring small concentrations of [125]Sb accurately.

Because very little europium, which is relatively involatile under oxidizing conditions, has been released in previous tests in steam, very low release was expected in this test in air and steam. A small amount of [154]Eu (~0.04% of the fuel inventory) was measured on furnace components, but only trace amounts (~0.001%) were detected on the filters. As shown in Table 3.4, 49% of the released [125]Sb was found deposited on ceramic surfaces in the outlet region of the furnace, where temperatures were 1200 to 2000 K during the test. While ^{60}Co is not a fission product, but rather an activation product resulting from cobalt impurity in the Zircaloy cladding, it was measured to provide information about the behavior of structural materials. The distribution data shown in Table 3.4 indicate that some 74% of the cobalt released from the fuel specimen deposited in the furnace, and that ~2/3 of the cobalt released from the furnace was in aerosol

form. As would be expected, 70% of the release occurred during Test Phase C, the 20-min period at ~2300 K.

## 3.2 Analysis for Iodine

Since iodine has no long-lived, gamma-emitting nuclides, analytical methods other than gamma spectrometry must be used. Neutron activation of [129]I to [130]I, which can be counted easily, is a proven, sensitive technique. Because the normally occurring iodine forms dissolve readily in basic solutions to form stable iodides, each of the collector components from this test were leached with $NH_4OH$ to remove this iodine for analysis. After chemical treatment of small aliquotes of the leach solution to separate the halides (especially iodine) from the other fission products, the samples were loaded onto ion-exchange media and irradiated briefly. After an optimum decay period, the samples were analyzed for the resulting 12.5-h [130]I.

The iodine data, for Tests VI-6 and VI-7, are summarized in Table 3.5. The tests experienced similar time/temperature histories (20 min each at 2000 and 2300 K) but were exposed to different oxidizing atmospheres. While Test VI-7 used limited steam plus air throughout the test period, Test VI-6 was heated to 2320 K in hydrogen, then hydrogen flow was stopped and steam was introduced later in the test. The results show that total iodine release was greater in the test with heatup in hydrogen followed by steam (71.3% in Test VI-6) than in the test in steam + air (41.5% in Test VI-7). Furthermore, a much larger fraction of the released iodine was retained in the furnace in pure steam (34.2% in VI-6 vs 4.17% in VI-7).

Some iodine forms (organic iodides, elemental iodine, or hydrogen iodide) may pass through the TGTs, penetrate the filters, and adsorb onto the heated charcoal in the filter packages. For this reason, the charcoal cartridges were analyzed for [129]I by direct neutron activation also. The results of these analyses, presented in Table 3.6, show that almost all (~98%) of this volatile iodine was collected on the first of the four cartridges during Test Phase A. The total fraction of the released iodine that was collected on the charcoal in Test VI-7 (0.28%) was similar to most previous tests, which have averaged <0.5%. The fractions of iodine found in vapor and aerosol forms, as well as their mass ratios, are shown in Table 3.7.

Table 3.3  Physical forms of cesium released from furnace in Test VI-7

| Collection period | Amount in designated form (% or inventory) | | |
| --- | --- | --- | --- |
| | Vapor | Aerosol | Total |
| A | 24.5 | 32.7 | 57.2 |
| B | 6.6 | 10.0 | 16.6 |
| C | 12.5 | 13.8 | 26.3 |
| Total A+B+C | 43.6 | 56.5 | 100 |

Table 3.4 Fractional releases and distributions of antimony and
cobalt (from cladding) in Test VI-7[*]

| Location | [125]Sb | | | [60]Co | | |
|---|---|---|---|---|---|---|
| | $\mu$Ci | % of inventory | % of released | $\mu$Ci | % of inventory | % of released |
| **Furnace components** | | | | | | |
| First ZrO$_2$ plug | 144 | 0.64 | 1.24 | 1560.0 | 19.36 | 65.00 |
| Second ZrO$_2$ plug | 5497 | 24.33 | 47.25 | 205.0 | 2.54 | 8.54 |
| Exit region | 66 | 0.29 | 0.57 | 5.5 | 0.07 | 0.23 |
| Furnace total | 5707 | 25.26 | 49.06 | 1770.5 | 21.97 | 73.77 |
| **Train A** | | | | | | |
| TGT A | 0 | 0.00 | 0.00 | 26.0 | 0.32 | 1.08 |
| TGT, filter line | 0 | 0.00 | 0.00 | 7.3 | 0.09 | 0.30 |
| First prefilter | 0 | 0.00 | 0.00 | 44.3 | 0.55 | 1.85 |
| Second prefilter | 0 | 0.00 | 0.00 | 0.7 | 0.01 | 0.03 |
| HEPA filters | 0 | 0.00 | 0.00 | 0.0 | 0.00 | 0.00 |
| Total in Train A | 0 | 0.00 | 0.00 | 78.3 | 0.97 | 3.26 |
| **Train B** | | | | | | |
| TGT B | 0 | 0.00 | 0.00 | 40.0 | 0.50 | 1.67 |
| TGT, filter line | 200 | 0.89 | 1.72 | 11.8 | 0.15 | 0.49 |
| First prefilter | 826 | 3.66 | 7.10 | 59.4 | 0.74 | 2.48 |
| Second prefilter | 50 | 0.22 | 0.43 | 4.1 | 0.05 | 0.17 |
| HEPA filters | 2 | 0.01 | 0.02 | 0.2 | 0.00 | 0.01 |
| Total in Train B | 1078 | 4.77 | 9.27 | 115.5 | 1.43 | 4.81 |
| **Train C** | | | | | | |
| TGT C | 1424 | 6.30 | 12.24 | 152.0 | 1.89 | 6.33 |
| TGT, filter line | 689 | 3.05 | 5.92 | 35.1 | 0.44 | 1.46 |
| First prefilter | 2620 | 11.60 | 22.52 | 237.0 | 2.94 | 9.88 |
| Second prefilter | 78 | 0.35 | 0.67 | 9.8 | 0.12 | 0.41 |
| HEPA filters | 37 | 0.16 | 0.32 | 2.1 | 0.03 | 0.09 |
| Total in Train C | 4848 | 21.46 | 41.67 | 436.0 | 5.41 | 18.17 |
| Total released from fuel | 11633 | 51.48 | 100.00 | 2400 | 29.78 | 100.01 |
| Total in fuel (after test) | 10962 | 48.52 | | 5659 | 70.22 | |

[*]Inventories based on measured data: 22.595 $\mu$Ci [125]Sb and 8.059 $\mu$Ci [60]Co.

Table 3.5 Fractional releases and distributions of iodine in Tests VI-6 and VI-7[*]

| Location | Test VI-6 | | | Test VI-7 | | |
|---|---|---|---|---|---|---|
| | μg | % of inventory | % of released | μg | % of inventory | % of released |
| **Furnace Total** | 2913 | 24.35 | 34.2 | 353 | 1.73 | 4.17 |
| **Train A** | | | | | | |
| TGT A | 396 | 3.31 | 4.64 | 2031 | 9.94 | 23.9 |
| TGT to filter tube | 246 | 2.06 | 2.89 | 577 | 2.82 | 6.79 |
| Prefilters | 1293 | 10.81 | 15.2 | 1791 | 8.77 | 21.1 |
| HEPA filters | 0 | 0.0 | 0.0 | 0 | 0.0 | 0.0 |
| Charcoal | 339 | 2.83 | 3.97 | 80.2 | 0.39 | 0.94 |
| Total in Train A | 2273 | 19.00 | 26.7 | 4479 | 21.9 | 52.7 |
| **Train B** | | | | | | |
| TGT B | 234 | 1.96 | 2.75 | 836 | 4.09 | 9.85 |
| TGT to filter tube | 18 | 0.15 | 0.21 | 160 | 0.78 | 1.88 |
| Prefilters | 177 | 1.48 | 2.08 | 543 | 2.66 | 6.41 |
| HEPA filters | 0 | 0.0 | 0.0 | 0 | 0.0 | 0.0 |
| Charcoal | 64 | 0.54 | 0.75 | 0.74 | 0.004 | 0.01 |
| Total in Train B | 493 | 4.12 | 5.78 | 1540 | 7.54 | 18.2 |
| **Train C** | | | | | | |
| TGT C | 813 | 6.80 | 9.54 | 549 | 2.69 | 6.48 |
| TGT to filter tube | 123 | 1.03 | 1.44 | 525 | 2.57 | 6.19 |
| Prefilters | 1487 | 12.43 | 17.4 | 1038 | 5.08 | 12.23 |
| HEPA filters | 0 | 0.0 | 0.0 | 0 | 0.0 | 0.0 |
| Charcoal | 428 | 3.58 | 5.02 | 0.96 | 0.005 | 0.01 |
| Total in Train C | 2851 | 23.83 | 33.4 | 2113 | 10.34 | 24.9 |
| Total released from fuel | 8531 | 71.30 | | 8486 | 41.53 | |

[*]Total iodine inventories based on ORIGEN2 (calculated) data: VI-6 contained 11.96 mg and VI-7 contained 20.43 mg.

Table 3.6  Volatile iodine collected in Test VI-7

| Sample No. | Volatile iodine[*] | |
| --- | --- | --- |
| | Mass ($\mu$g) | Percent of inventory |
| AC1 | 79.9 | 2.73E$-$1[**] |
| AC2 | 0.186 | 6.3E$-$4 |
| AC3 | 0.071 | 2.4E$-$4 |
| AC4 | ND[†] | |
| BC1 | 0.74 | 2.5E$-$3 |
| BC2 | ND[†] | |
| BC3 | ND[†] | |
| BC4 | ND[†] | |
| CC1 | 0.92 | 3.1E$-$3 |
| CC2 | 0.037 | 1.3E$-$4 |
| CC3 | ND[†] | |
| CC4 | ND[†] | |
| Totals | 81.9 | 2.80E$-$1 |

[*]As determined by measurements of $^{129}$I.
[**]Exponential notation:  2.73E-1 = 2.73 $\times$ 10$^{-1}$.
[†]ND = not detected.

Table 3.7 Comparison of physical forms of iodine and
cesium released to collection trains in Test VI-7

| Collection period | Fraction in designated form (% of element released from furnace)[*] | | | | | | | | |
| | Vapor | | | Aerosol | | | Total | | |
| | I | Cs | Cs/I | I | Cs | Cs/I | I | Cs | Cs/I |
| --- | --- | --- | --- | --- | --- | --- | --- | --- | --- |
| A | 25.9 | 24.5 | 0.95 | 29.1 | 32.7 | 1.12 | 55.1 | 57.2 | 1.04 |
| B | 10.3 | 6.6 | 0.64 | 8.8 | 10.0 | 1.14 | 18.9 | 16.6 | 0.88 |
| C | 6.8 | 12.5 | 1.84 | 19.2 | 13.8 | 0.72 | 26.0 | 26.3 | 1.01 |
| Total A+B+C | 43.0 | 43.6 | 1.01 | 57.1 | 56.5 | 0.99 | 100 | 100 | 1.00 |

[*]Based on total inventory in the fuel, 39.8% of the iodine and 4.1% of the cesium were released from the furnace.

## 3.3 Thermal Gradient Tube Deposits

The three TGT liners were made by rolling 0.003-in.-thick platinum foil into tubes. These liners were inserted into the surrounding Inconel TGTs and then removed after the test and examined. During the test, each of the 36-cm-long TGT liners had been subjected to maximum temperatures of ~800°C at the inlet end. The TGT temperatures declined approximately linearly to ~150°C at the exit end.

The collection of cesium on the TGT liners was monitored during the test by continuous gamma spectrometry of the $^{134}$Cs and $^{137}$Cs. The $^{137}$Cs profiles for the three TGTs, as well as the temperature profile along the TGTs, are shown in Figure 3.2. The larger amounts of $^{137}$Cs in TGT A, and its concentration in the central region at deposition temperatures of 400 to 700°C, are apparent. Small amounts of $^{60}$Co (an activation product) were present in both TGT B and TGT C, and a low level of $^{125}$Sb was measured in most areas of TGT C, as shown in Figure 3.3.

Upon opening the liners, the internal deposits were found to be generally gray in color and uniformly distributed. Liner B contained some thin brown deposits, but the heaviest deposits were found in Liner C, which was embrittled at the inlet end. Potential causes for such embrittlement of the inlet end of the platinum liner are believed to be related to alloying with elemental forms of tin (from the Zircaloy cladding) or tellurium and/or antimony (fission products), all of which had maximum release rates during Test Phase C.

## 3.4 Masses of Deposits in TGTS and on Filters

The filters and TGT liners were weighed before and after the test to determine the mass of material collected. Most of the material deposited in the TGT liners is believed to be a result of vapor condensation, and the material deposited on the filters probably was transported primarily as aerosol. Immediately after disassembly of the filter packages, the filters were inspected and packaged for weighing. Although the prefilters exhibited light deposits, no deposits were visible and no weight changes were observed for the HEPA filters, indicating efficient collection of the aerosols by the prefilters.

The masses of material collected at the various locations are summarized in Table 3.8 and illustrated in Figure 3.4. As would be expected, the greatest mass was collected during Phase C, the highest temperature period. For similar times and temperatures, the total mass of collected material (0.888 g) was somewhat less in Test VI-7 than in the pure steam atmosphere Test VI-2 (1.134 g), but much greater than in Test VI-6 (0.573), which was heated in hydrogen and then exposed to steam. The mass collected outside the furnace was 0.52% of the fuel specimen mass. As seen in previous tests in oxidizing atmospheres, the mass ratio of vapor to aerosol was about 1 to 2.

## 3.5 ICP-ES Analyses

Samples of the acidic leach solutions from the TGT liners, the filters, and other test components were submitted for analysis by inductively coupled plasma-emission spectrometry (ICP-ES). This technique is well suited for measuring several of the non-gamma-emitting fission product elements and uranium. Unfortunately, it is not useful for iodine analysis. The high levels of radiocesium in most of the samples, however, have often required dilutions (which reduced precision) to avoid excess radiation dose to the analyst.

As would be expected, major release fractions of these less-volatile elements were retained in the outlet end of the furnace where the time (Test Phase A, B, or C) of release and/or deposition cannot be determined. Furthermore, the largest fractions of these four elements that were released to the collection trains were found in Train C as shown in Table 3.9. Because of its well-known sensitivity to the effects of oxidizing conditions, most of the release of molybdenum is believed to have occurred after the cladding had been oxidized by the steam and air. Similar behavior was expected for ruthenium but is not shown by these data. (Because of the long decay time of the fuel, ~14 years, more accurate analysis by gamma spectrometry for $^{106}$Ru was not possible. In previous tests, gamma analysis for $^{106}$Ru has indicated much lower releases of ruthenium than has the ICP method used for ruthenium in Test VI-7.)

The observed behavior of these four less-volatile fission product elements is not in consistent agreement with the CORSOR model and with other experimental data.[18] The agreements for strontium and barium were reasonably good, but the indicated releases of molybdenum and
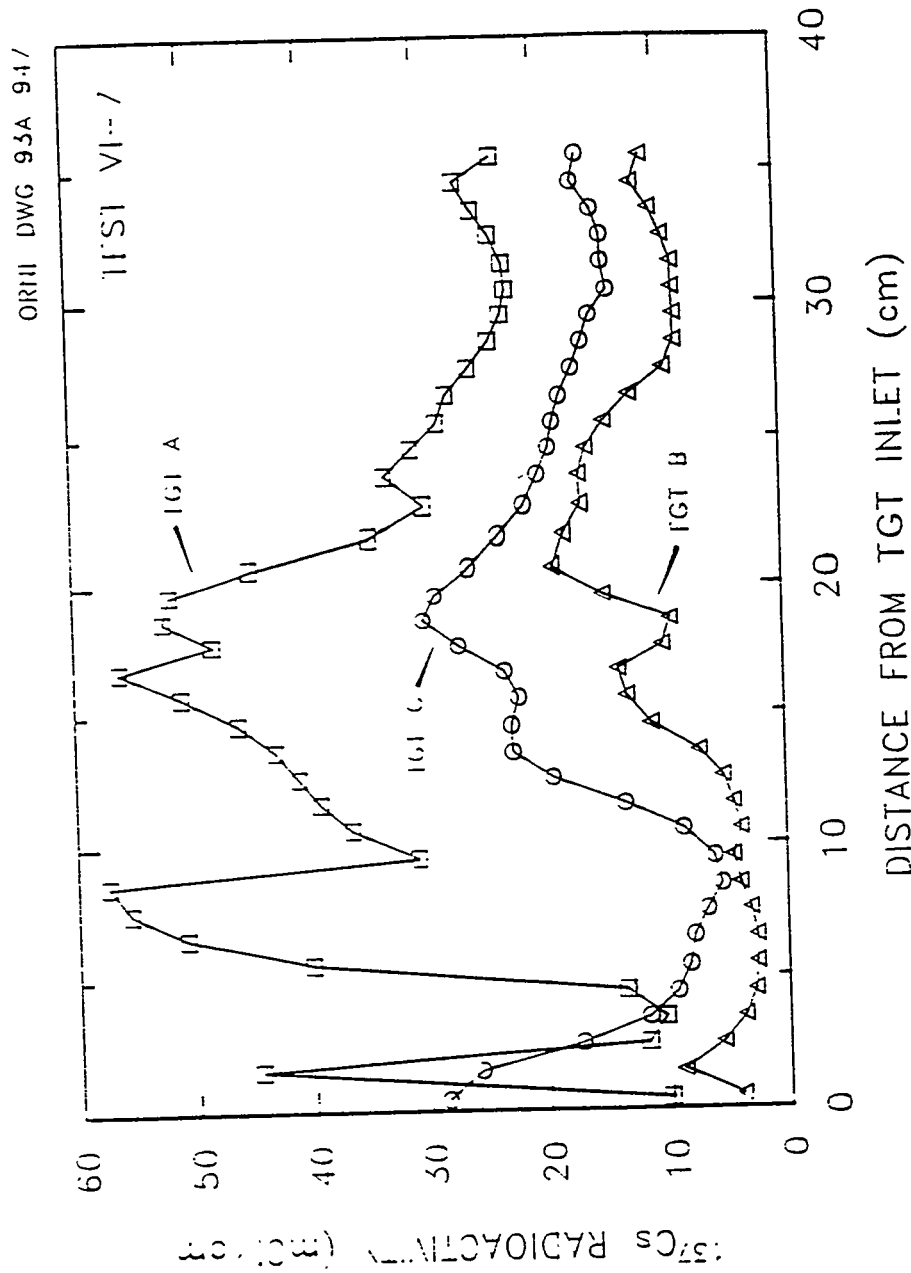
Figure 3.2  Distribution of $^{137}$Cs in TGT liners of Test VI-7
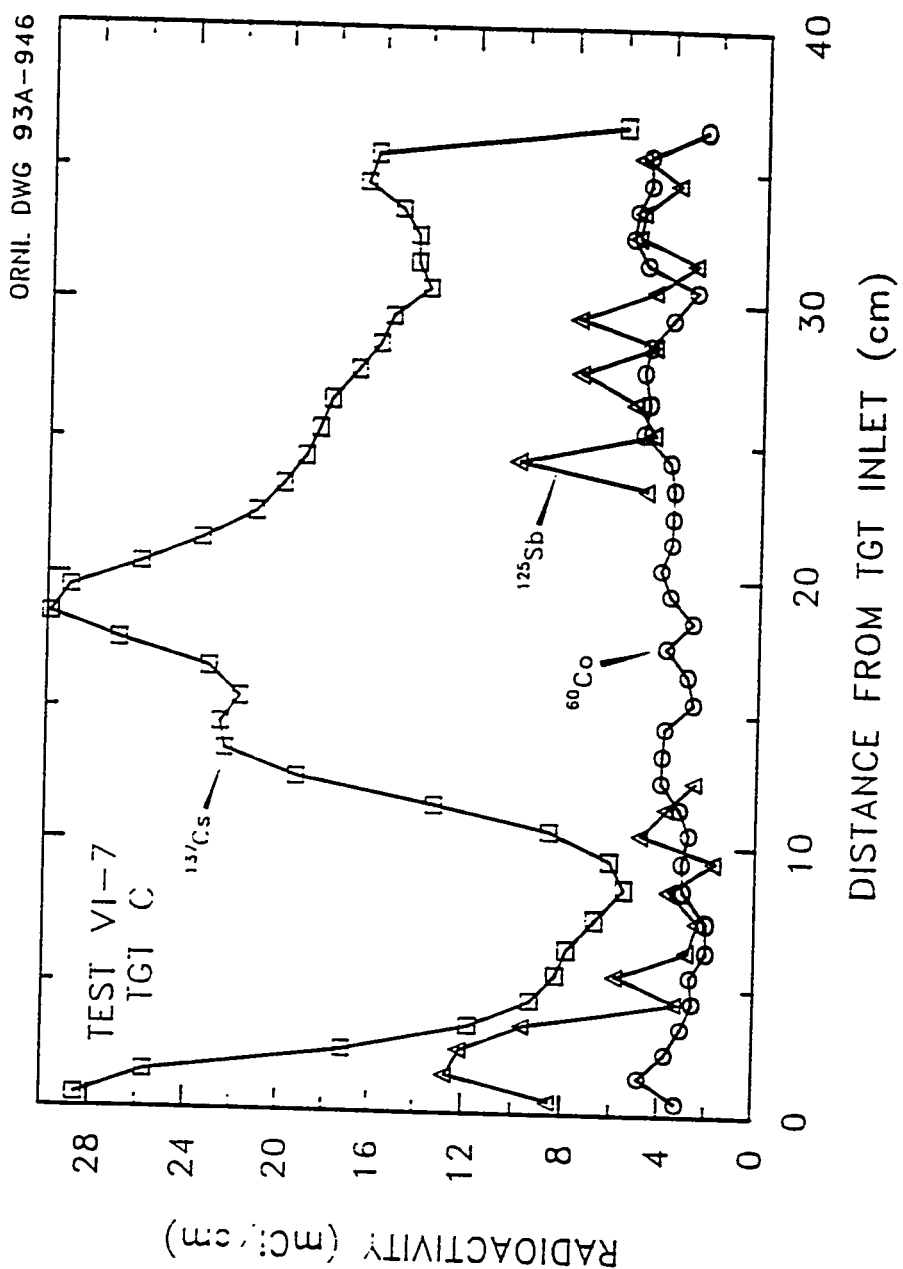
Figure 3.3    Distributions of $^{137}$Cs, $^{125}$Sb, and $^{60}$Co in TGT C liner of Test VI-7

Table 3.8 Vapor and aerosol deposits in Test VI-7

| | Weight of deposits (g)[*] | | | |
| | Train A | Train B | Train C | Total |
|---|---|---|---|---|
| TGT | 0.108 | 0.012 | 0.206 | 0.326 |
| Filters | | | | |
| Prefilter 1 | 0.149 | 0.075 | 0.326 | 0.550 |
| Prefilter 2 | 0.004 | 0.004 | 0.004 | 0.012 |
| HEPAs | 0.000 | 0.000 | 0.000 | 0.000 |
| Total filters | 0.153 | 0.079 | 0.330 | 0.562 |
| Total deposits (TGTs and filters) | 0.261 | 0.091 | 0.536 | 0.888 |

[*]Precision = ±0.003 g.
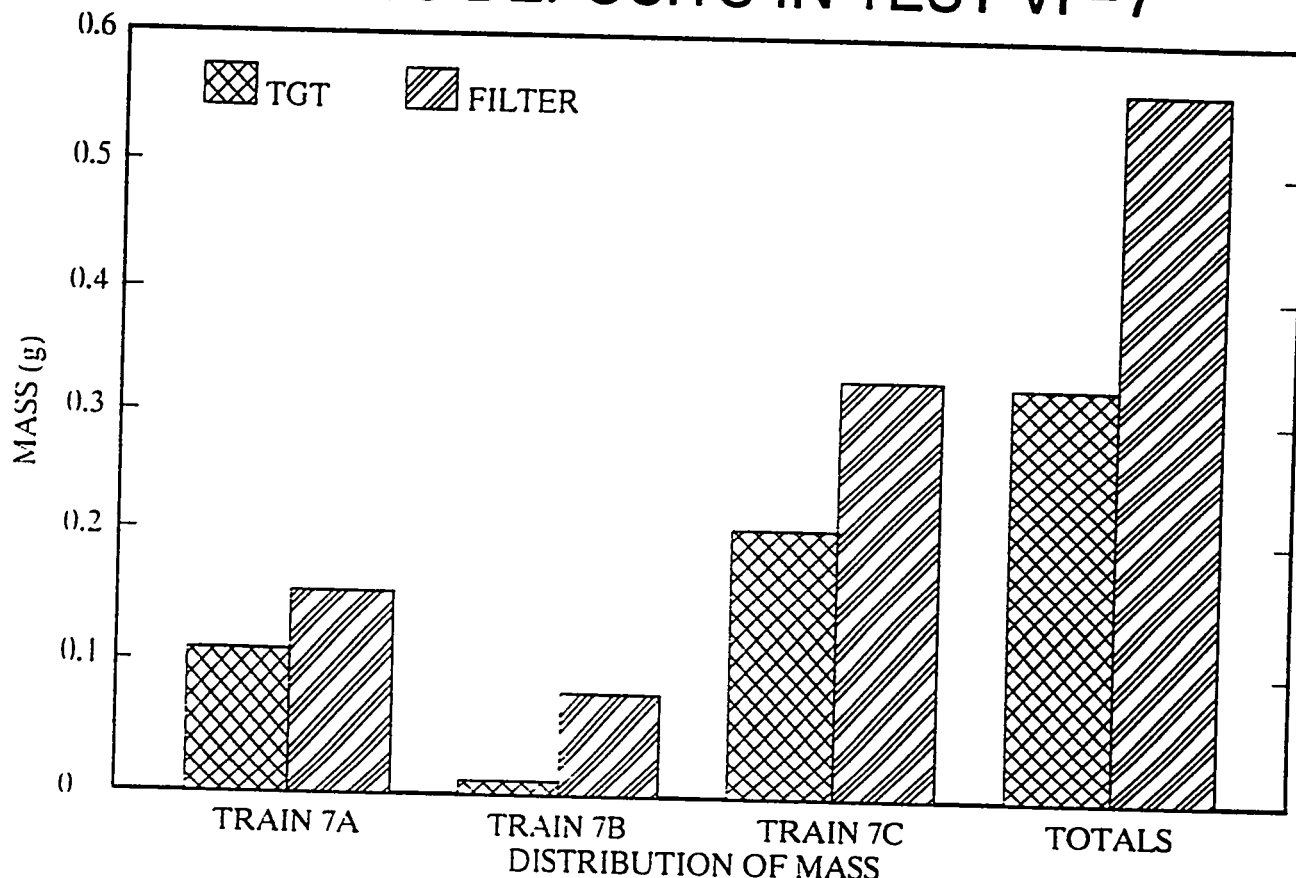
Figure 3.4 Mass distribution to the collection system of material released in Test VI-7

### Table 3.9 Release of low-volatility fission products in Test VI-7

| Collection location | Fractional release from fuel (%)[*] | | | |
|---|---|---|---|---|
| | Sr | Mo | Ru[**] | Ba |
| Furnace | 1.09 | 1.40 | 1.54 | 2.44 |
| Train A | 0.021 | 0.058 | 0.441 | 0.587 |
| Train B | 0.018 | 0.090 | 0.285 | 0.324 |
| Train C | 0.038 | 3.79 | 0.285 | 0.707 |
| Totals | 1.16 | 5.33 | 2.55 | 4.05 |

[*]Fuel inventories were calculated by ORIGEN2.
[**]Values shown for ruthenium are not measured values. Although ruthenium was detected in many samples, the concentrations were not sufficient for accurate measurement. Consequently, we assumed 50% of the minimum quantities required for accurate measurements.

ruthenium were much lower than expected. Unfortunately, it was not possible to determine the extent of tellurium release. While a significant tellurium release would be expected late in the test, no tellurium was detected.

# 3.6 Modeling of Volatile Fission Product Release

Because the $^{85}$Kr, $^{134}$Cs, and $^{137}$Cs were collected and measured on line at 1-min intervals during the test, calculation of the minute-by-minute release rates was readily accomplished. As in previous tests, the release behaviors of krypton and cesium were similar.

The on-line data for krypton and cesium were used to calculate the minute-by-minute release rate and diffusion coefficients during Test VI-7. The cesium release rate coefficients, plotted as a function of temperature during the test, are shown in Figure 3.5. The clusters of points at 2000 K and 2300 K indicate the 20-min periods at constant temperature. It is apparent that the resulting curve lies above the CORSOR-M curve below 2000 K but below CORSOR-M at higher temperatures. The corresponding Test VI-7 diffusion coefficients for cesium are compared with the ORNL Booth Model in Figure 3.6. While the data deviate from the curve in the same manner (i.e., higher below 2000 K and lower above that temperature), the agreement with the ORNL Booth Model appears to be better than with CORSOR-M. The cesium release rate coefficients for all ORNL VI tests, plotted in Figure 3.7, show that Test VI-7 data lie within the envelope of data. Because the curve for the CORSOR-M model lies slightly above most ORNL-VI data, we conclude that it is conservative for cesium and other volatile fission products.

## 3.7 Cladding Oxidation

As indicated in Figure 2.1, the test atmosphere (a mixture of air, steam, and helium in Test VI-7) entered the furnace at the bottom and flowed upward past the fuel specimen. Hence, conditions were most oxidizing at the bottom end of the specimen and decreased with elevation as the oxygen in the air and the steam reacted with the hot Zircaloy cladding. In fact, during the early part of the test, all oxidizing components in the atmosphere should

have been consumed, and the steam replaced by hydrogen, before reaching the top end of the specimen.

To investigate the characteristics of the atmosphere and the extent of cladding oxidation as functions of test time and fuel specimen location, calculations were carried out using a simple model reported by Yamashita.[19] In this model, oxidation of the two end caps and 11 cladding nodes in between was considered, and the results are presented in Figures 3.8 and 3.9. The vertical movement of the oxidation front along the fuel specimen is illustrated by the calculated oxidation profiles in Figure 3.8. These profiles, covering test times from 60 to 85 min, indicate that at 60 min the maximum extent of cladding oxidation was 40% over the lower five cladding nodes.

The metallographic examination of two radial sections of the fuel specimen provided additional information and generally corroborated the oxidation calculations. In addition, the observations were useful in interpreting the fission product release and distribution results. One radial section from the lower end of the fuel specimen showed complete, typically uniform oxidation, as illustrated in Figure 3.10.

Some adherence of $UO_2$ to the cladding and limited interaction is apparent at the fuel-cladding interface. A section from the upper end, while heavily oxidized, exhibited a quite different appearance (see Figure 3.11). The oxide was less uniform, with numerous voids, areas of porosity, and inclusions, suggesting that conditions changed during the test. Some mid-wall areas retained metallic phases, apparently enriched in tin driven by the oxidation front, as seen in Figure 3.12. Unidentified bright phases (Figure 3.11), believed to be zirconium nitride formed by reactions with nitrogen in the air atmosphere, were observed in many locations. The less uniform and more porous appearance of the oxidized cladding near the top end of the specimen suggested that the limited steam dominated the reaction processes and was consumed near the bottom (entrance) end, leaving a gas mixture relatively rich in air and hydrogen to react with the upper regions. In addition, the gas mixture would have changed as the oxidation front moved up the specimen, as illustrated in Figures 3.10 and 3.11. (It should be noted that the results of oxidation calculations displayed in Figures 3.8 and 3.9 assumed, based on a limited review of the literature, equal reaction rates between the cladding and the oxidizing air and steam.)
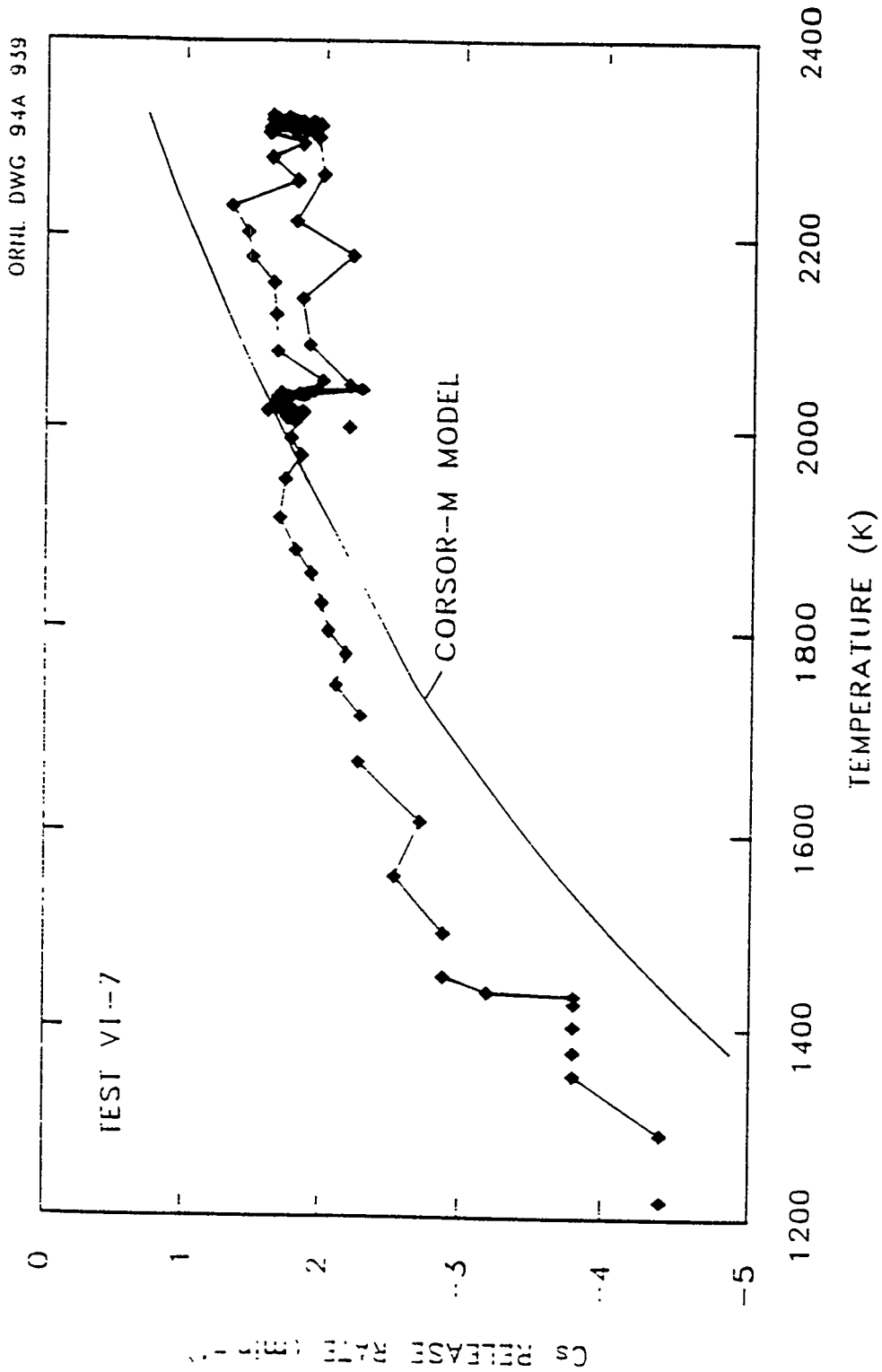
**Figure 3.5** Release rate coefficients for cesium in Test VI-7, plotted as a function of temperature. Note clusters of points at 200 and 2300 K, the periods at constant temperature.
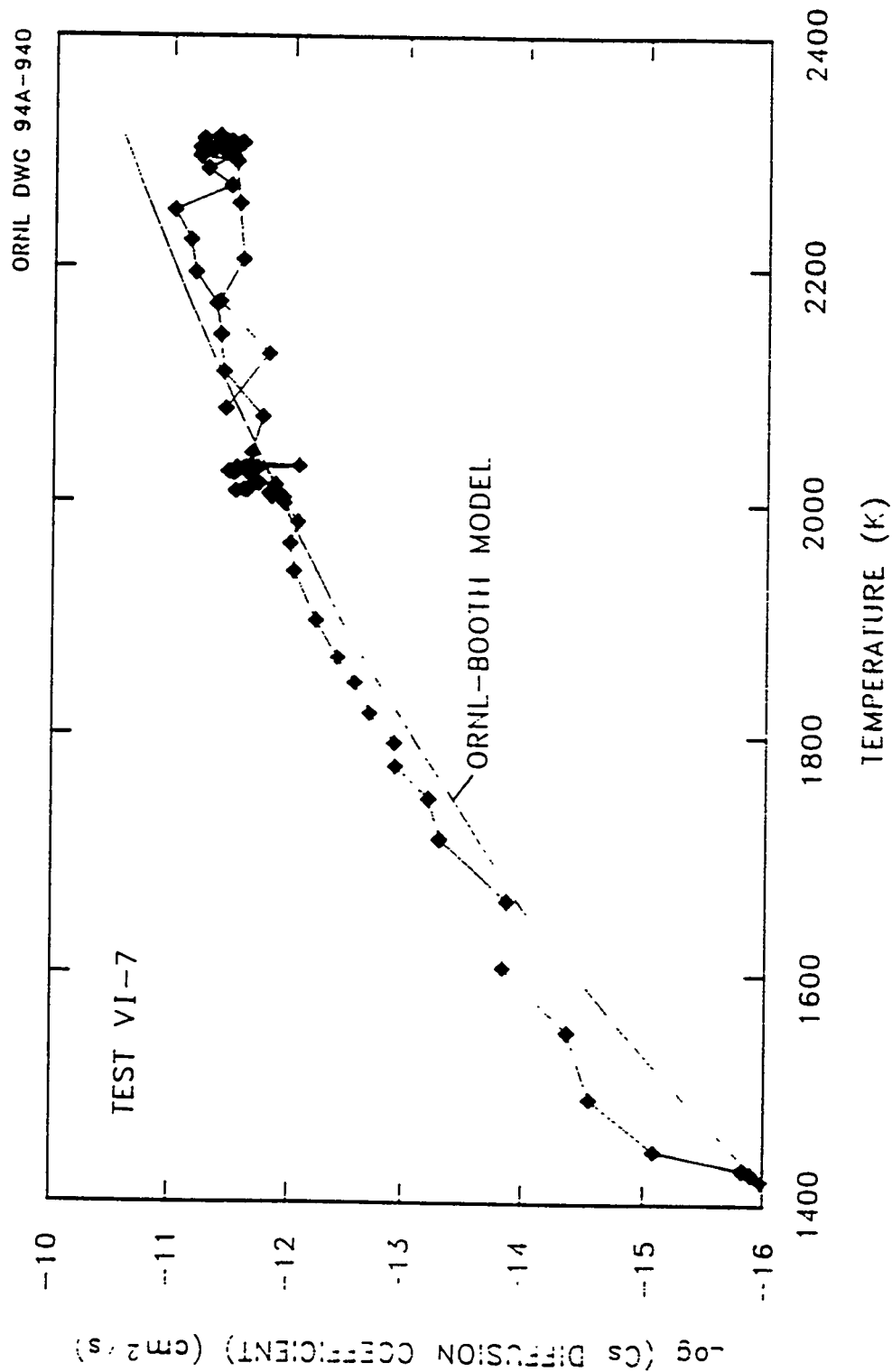
Figure 3.6 Diffusion coefficients for cesium release in Test VI-7. Note clusters of points at 2000 and 2300 K, the periods at constant temperature
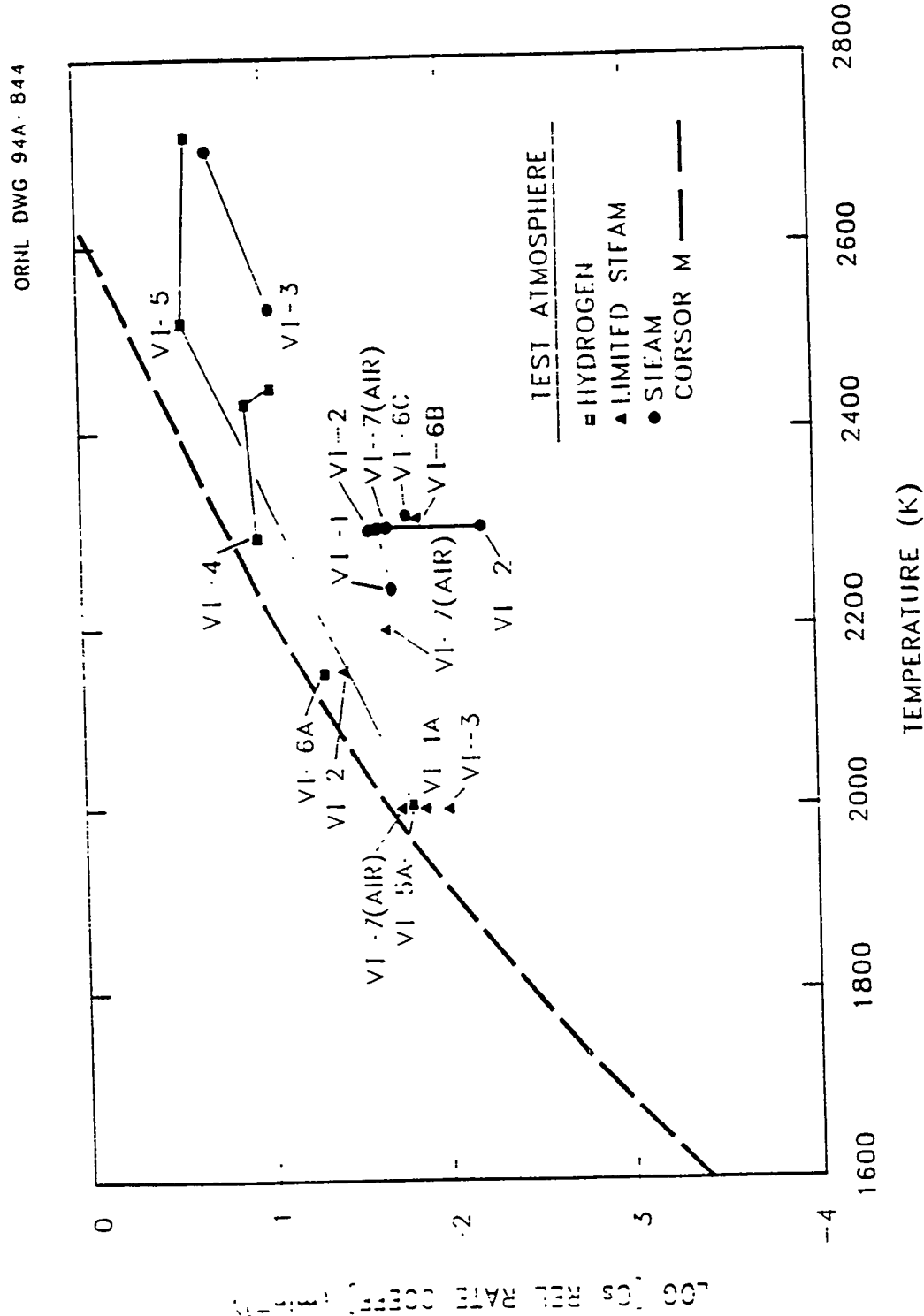
Figure 3.7   Cesium release rate coefficients for ORNL VI tests.   Note that values for Test VI-7 lie below
CORSOR-M model and within the envelope of ORNL data

38
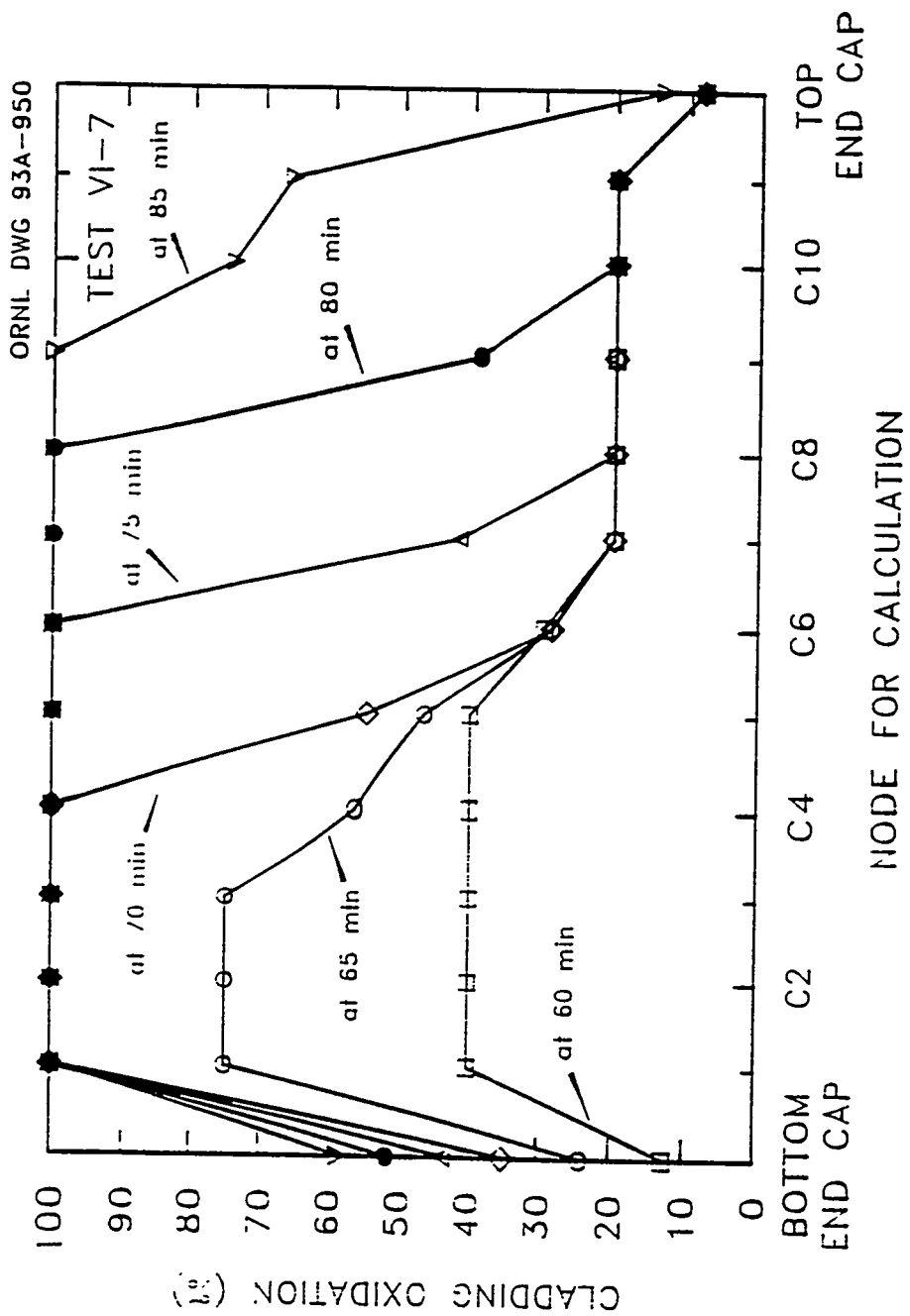
**Figure 3.8** Successive oxidation profiles at test times of 60 to 85 min as calculated for Test VI-7
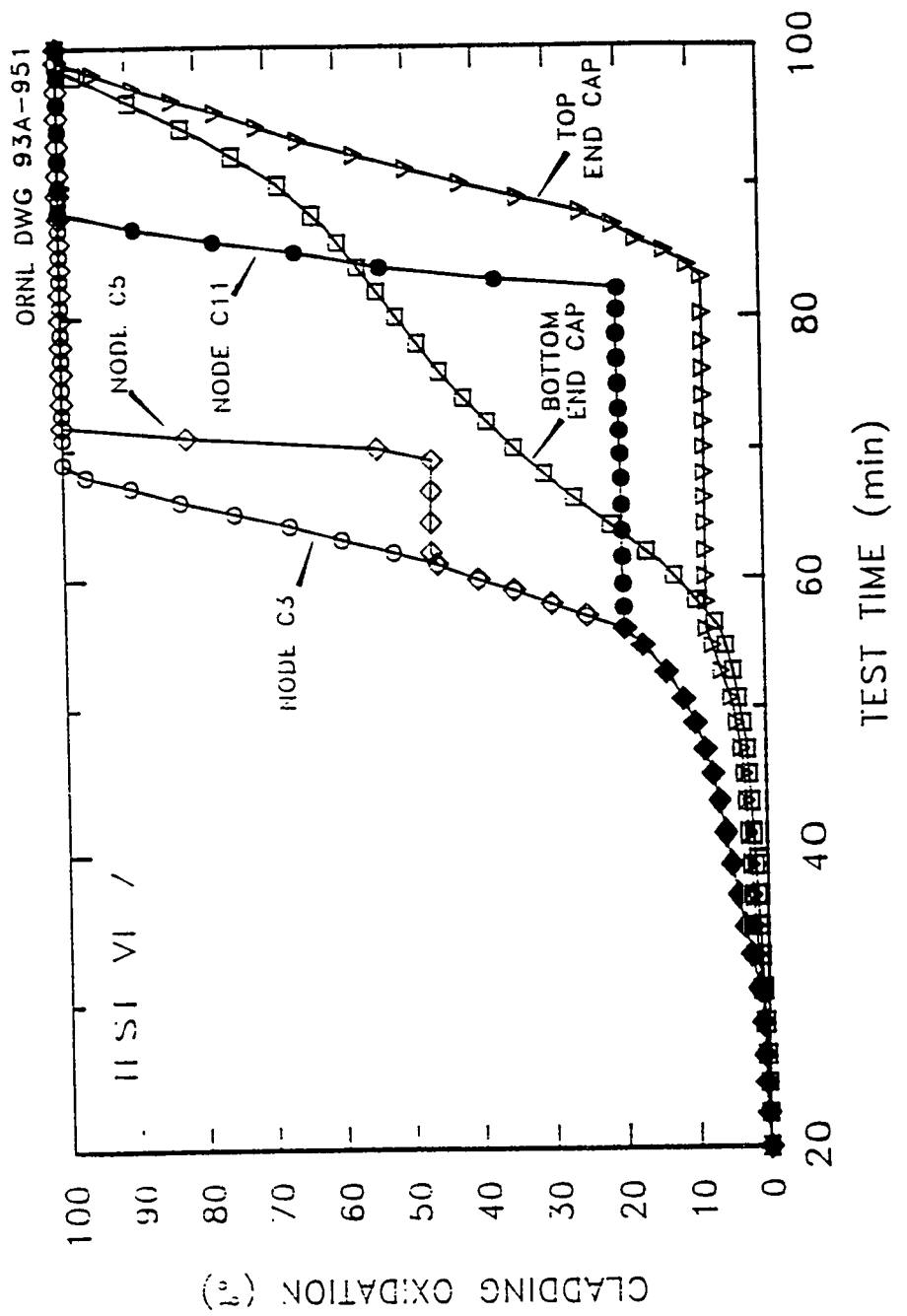
Figure 3.9  Calculated extent of Zircaloy oxidation for selected locations in Test VI-7

UO$_2$

ZrO$_2$

Clad OD

200 um          100X
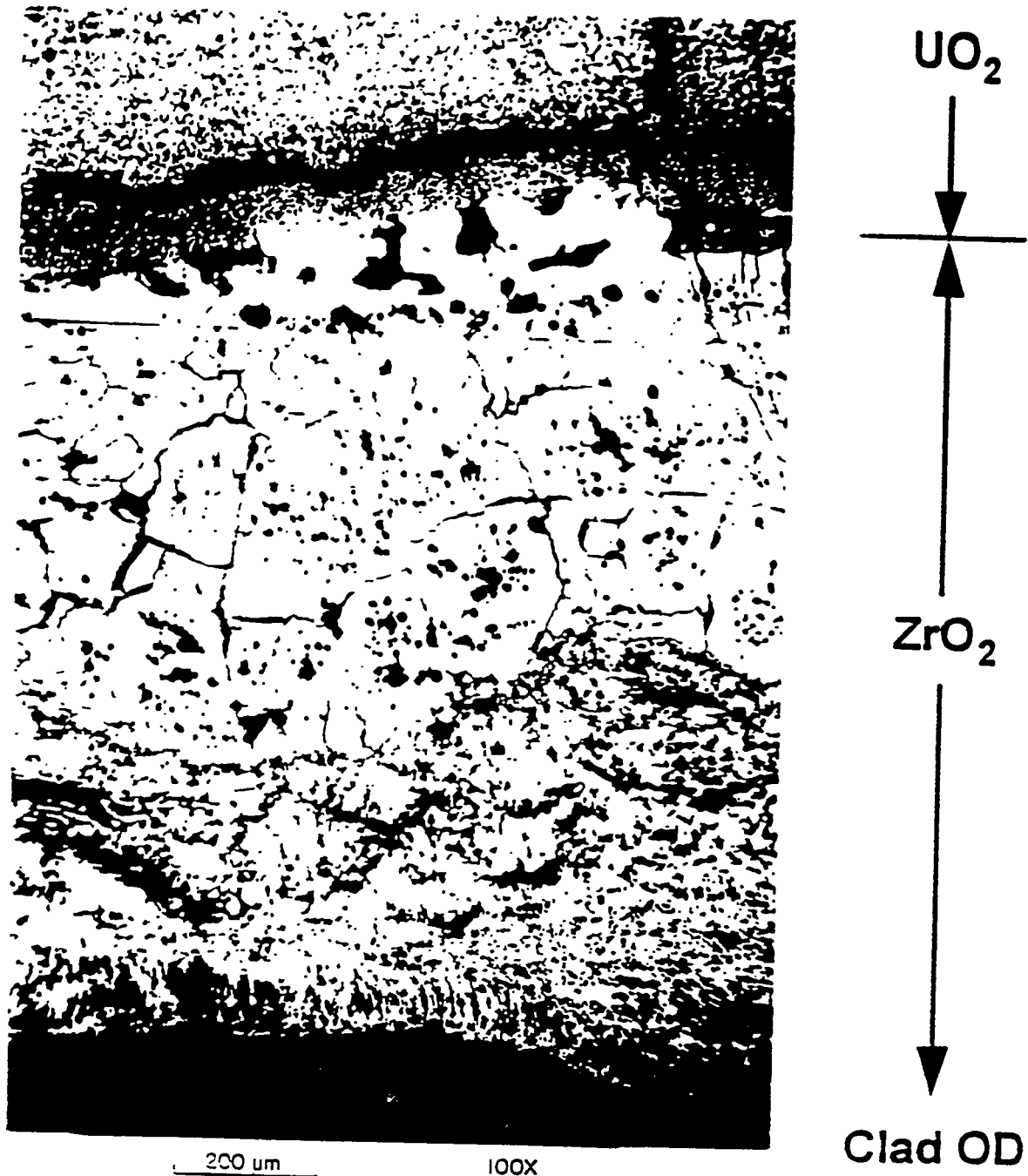
Figure 3.10  Fuel-cladding section from near the bottom end of Test VI-7 showing uniformly oxidized cladding and fuel-cladding interface

**Clad ID**

**Clad OD**

200 um     100X
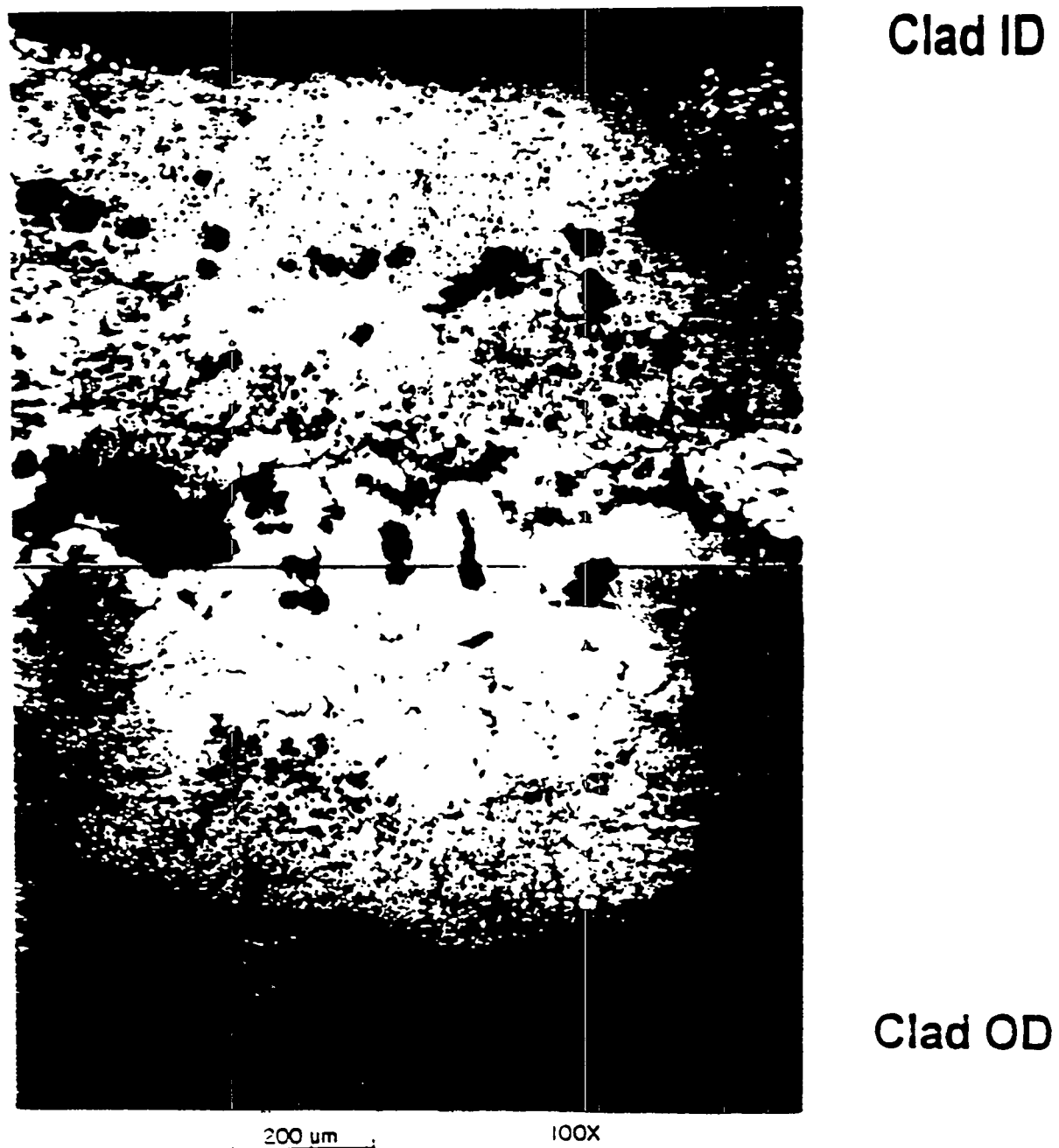
Figure 3.11  Radial section of cladding from near the top end of Test VI-7; note non-uniform oxidation, voids, and inclusions in the cladding

**Clad ID**

**Clad OD**

200 um        100X

Figure 3.12 Radial section of cladding from near the top end of Test VI-7 showing bright phases of metallic material at mid-wall

The heavy, uniform oxide near the bottom end is typical
of oxidation by steam, whereas the porous, irregular layer
of oxide and other phases and inclusions near the top end
suggest oxidation by air. Consequently, the $UO_2$ fuel
should have been most oxidized at the bottom end, with
an oxidation gradient declining with elevation; these
conditions correspond to observed release gradients along
the fuel specimen for cesium and antimony (see
Figure 3.1) The good agreement of these results of
metallographic examination support the predictions of the
Yamashita model discussed above and verify the validity
of the model.[19]

# 4 Comparison of Release Data with Previous Results

The fission product release data from Test VI-7 have been compared with the results from earlier experiments. Because it was similar to Test VI-1 except for the addition of air into the test atmosphere, we were particularly interested in comparing the results from these two tests.

The integral release data for eight fission product elements from Test VI-7 are compared with the results from six previous tests (VI-1 through VI-6) in Table 4.1. Comparison of the data from these tests suggests that the presence of air in the atmosphere results in slightly higher releases for most elements. Moderate oxidation of the $UO_2$ over the lower half of the specimen could explain the observed gradient in fission product release (see Figure 3.1). The indicated differences in molybdenum and ruthenium release (shown in Table 4.1) are apparent contradictions. However, the wide ranges in values for molybdenum and ruthenium release indicate relatively low levels in precision (and confidence) in the data for these elements.

On the other hand, the fractional releases of krypton and cesium were always similar, except for the lower krypton value for Test VI-2, where some of the gas was known to have been lost. Furthermore, krypton and cesium release values exhibited a general increase with test temperature, reaching ~100% at 2700 K. No significant influence of the reactive atmospheres, steam and hydrogen, on the release of these highly volatile elements was apparent. Although the release values are somewhat lower in all cases, probably because of difficulties in complete sampling, we believe that iodine behaves similarly to krypton and cesium.

With regard to atmospheric effects on the less volatile species, the recent data supported the conclusions drawn from earlier results.[20,21] The release behaviors of Sb, Mo, Ba, and Eu, on the other hand, showed a clear influence of the reactive atmospheres, and these atmospheric effects became more exaggerated at the highest temperature, 2700 K. Much higher releases of Sb and Mo were observed in steam, whereas Ba, Sr, and Eu releases were higher in hydrogen. In conclusion, the behaviors of these elements in Test VI-7 were found to be generally consistent with their chemical characteristics and with data from previous tests.

Comparison of the total masses of material released in all VI tests, summarized in Table 4.2, shows that at 2300 K, Test VI-7 release appears somewhat low. Test VI-1, heated at the same time/temperature conditions, released 1.173 g, some 32% more, or 1.2% of specimen mass vs only 0.79% of the VI-7 mass. It was not possible, unfortunately, to obtain mass spectrometric analyses for the Test VI-7 samples to determine more about the differences in composition. Comparing the ratios of TGT/filter masses (Table 4.2) shows that, in Test VI-7, a greater fraction of material was collected on the TGTs than in earlier oxidizing tests, apparently an effect of the air atmosphere.

Table 4.1 Conditions and results for vertical (VI series) fission product release tests

| Parameter | Test number | | | | | | |
|---|---|---|---|---|---|---|---|
| | VI-1 | VI-7 | VI-2 | VI-6 | VI-3 | VI-4 | VI-5 |
| **Fuel specimen** | Oconee | Monticello | BR3 | BR3 | BR3 | BR3 | BR3 |
| Burnup, MWd/kg | 40 | 40 | 44 | 42 | 44 | 47 | 42 |
| In pile Kr release, % | 0.7 | ~2 | ~2 | ~2 | ~2 | ~5 | ~2 |
| **Test conditions** | | | | | | | |
| Test temperature, K | 2020, 2300* | 2025, 2310* | 2300 | 2310 | 2000, 2700* | 2440 | 2000, 2720* |
| Time at temp., min | 20, 20 | 20, 20 | 60 | 60 | 20, 20 | 20 | 20, 20 |
| Atmosphere** | Steam | Air, steam | Steam | Hydrogen, steam[c] | Steam | Hydrogen | Hydrogen |
| **Fractional release, %** | | | | | | | |
| $^{137}$Cs | 63 | 71 | 67 | 80 | 100 | 96 | 100 |
| $^{85}$Kr | 57 | 69 | >31 | 75 | 100 | 85 | 100 |
| $^{129}$I | 45 | 42 | 40 | 67 | 69 | 71 | 74 |
| $^{125}$Sb | 33 | 52 | 68 | 64 | 99 | 6.4 | 18 |
| $^{154}$Eu | 0 | 0.4 | 0 | 14 | ~0.01 | 19 | 57 |
| Ru | 0 | 2.6[b] | 0 | 0 | 5 | 0 | 0 |
| Te (approximate) | | 4.1 | | 63 | 99 | | 81 |
| Ba (approximate) | | 5.3 | 19 | 32 | 30 | 27 | 76 |
| Mo (approximate) | 43 | | 86 | 13 | 77 | 6.9 | 2.3 |
| U (approximate) | 0.009 | | 0.03 | 0.001 | 1.33 | | 0.015 |

*Some tests (VI-1, VI-3, VI-5, and VI-7) were conducted in two phases at two different temperatures.

**All tests included helium as a noncondensable carrier.

[c] Test VI-6 was heated to 2300 K in hydrogen then switched to a steam atmosphere.

[b] Data for ruthenium release from Test VI-7 appear to be significantly low, probably because of limited time of exposure to air.

Table 4.2 Mass release data for VI series tests

| Test phase | Fuel temperature (K) | Mass of material collected (g)* | | | Ratio TGT/filter |
|---|---|---|---|---|---|
| | | TGT | Filter | Total | |
| 1A | 2020 | 0.078 | 0.245 | 0.323 | 0.318 |
| 1B | 2020–2300 | 0.101 | 0.227 | 0.328 | 0.445 |
| 1C | 2300 | 0.225 | 0.297 | 0.522 | 0.758 |
| Totals | | 0.404 | 0.769 | 1.173 | 0.525 |
| 2A | 2300 | 0.057 | 0.188 | 0.245 | 0.303 |
| 2B | 2300 | 0.139 | 0.434 | 0.573 | 0.320 |
| 2C | 2300 | 0.085 | 0.231 | 0.316 | 0.368 |
| Totals | | 0.281 | 0.853 | 1.134 | 0.329 |
| 3A | 2000 | 0.061 | 0.308 | 0.369 | 0.198 |
| 3B | 2000–2700 | 0.380 | 1.094 | 1.474 | 0.347 |
| 3C | 2700 | 0.241 | 1.084 | 1.325 | 0.222 |
| Totals | | 0.682 | 2.486 | 3.168 | 0.274 |
| 4A | 2440 | 0.130 | 0.072 | 0.202 | 1.806 |
| 4B | 2440 | 0.002 | 0.093 | 0.095 | 0.022 |
| 4C | 2440 | 0.029 | 0.075 | 0.104 | 0.387 |
| Totals | | 0.161 | 0.240 | 0.401 | 0.671 |
| 5A | 2000 | 0.104 | 0.047 | 0.151 | 2.213 |
| 5B | 2000–2720 | 0.050 | 0.273 | 0.323 | 0.183 |
| 5C | 2720 | 0.030 | 0.177 | 0.207 | 0.169 |
| Totals | | 0.184 | 0.497 | 0.681 | 0.370 |
| 6A | 2310 | 0.100 | 0.036 | 0.136 | 2.778 |
| 6B | 2310 | 0.031 | 0.015 | 0.046 | 2.067 |
| 6C | 2310 | 0.161 | 0.230 | 0.391 | 0.700 |
| Totals | | 0.292 | 0.281 | 0.573 | 1.039 |
| 7A | 2025 | 0.108 | 0.153 | 0.261 | 0.706 |
| 7B | 2025–2310 | 0.012 | 0.079 | 0.091 | 0.152 |
| 7C | 2310 | 0.206 | 0.330 | 0.536 | 0.624 |
| Totals | | 0.326 | 0.562 | 0.888 | 0.580 |

*Precision = ±0.003 g.

# 5 Summary and Conclusions

This report summarizes all information available for Test VI-7 and compares the results with previous tests in this series. More extensive comparison and interpretation of all results are available.[8,13]

1. This was the first test in the VI series to include air in the test atmosphere. As expected, the mixture of air and limited steam caused complete oxidation of the Zircaloy cladding, and probably some oxidation of the $UO_2$ fuel near the inlet end. Near the outlet end of the fuel specimen, however, the cladding oxidation was extensive but not complete.

2. The measured integral release values for the fission products in this test were 69% for $^{85}$Kr, 42% for $^{129}$I, 71% for $^{137}$Cs, 52% for $^{125}$Sb, 0.40% for $^{154}$Eu, 1.2% for Sr, >2.6% for Ru, 4.1% for Ba, and 5.3% for Mo. Comparison of these results with data from previous tests indicated generally consistent behavior. Except for molybdenum and ruthenium, slightly greater releases were observed in air + steam (than in steam) at similar times and temperatures.

3. Fission product retention in the furnace varied widely. The retention fractions for cesium and iodine were fairly typical of previous tests: 10.4% for cesium and 4.2% for iodine. The retention of antimony, however, was 49% higher than was found in the steam oxidizing tests VI-1 through VI-3.

4. The total mass of deposits collected on the TGTs and the filters (0.888 g) was somewhat less than in other oxidizing tests at this temperature (2300 K).

5. Approximately 0.25% of the released iodine was collected on the charcoal filter cartridges, indicating it had been in a volatile form — $I_2$, HI, and/or $CH_3I$. This fraction is similar to values found for most of the VI tests; only VI-5 and VI-6 had a larger fraction of the released iodine in the charcoal.

6. The fractional releases of several less-volatile fission product elements were found to be significant, varying from 1.2% for strontium to 5.3% for molybdenum.

7. As in all previous tests, the release behavior of the volatile species (krypton and cesium) was very similar in Test VI-7. In addition, the diffusion coefficients for krypton and cesium calculated from on-line release data were in good agreement with the ORNL-Booth Model.

8. Metallographic examination of two radial sections from the fuel specimen verified that conditions had been somewhat more oxidizing at the bottom (inlet) end than at the top. In addition, the results indicated that calculations by a previously developed cladding oxidation model described the oxidation sequence with reasonable accuracy.

# 6 References

1. Osborne, M. F., J. L. Collins, and R. A. Lorenz, "Experimental Studies of Fission Product Release from Commercial LWR Fuel Under Accident Conditions," *Nucl. Technol.* 78(2):157–69 (August 1987).

2. Osborne, M. F., J. L. Collins, R. A. Lorenz, J. R. Travis, C. S. Webster, and T. Yamashita, "Data Summary Report for Fission Product Release Test VI-1," NUREG/CR-5339 (ORNL/TM-11104), June 1989.

3. Osborne, M. F., J. L. Collins, R. A. Lorenz, J. R. Travis, and C. S. Webster, "Data Summary Report for Fission Product release Test VI-2," NUREG/CR-5340 (ORNL/TM-11105), September 1989.

4. Osborne, M. F., J. L. Collins, R. A. Lorenz, J. R. Travis, C. S. Webster, S. R. Daish, H. K. Lee, T. Nakamura, and Y.-C. Tong, "Highlights Report for Fission Product Release Test VI-3," draft letter report to SFD Partners, July 1987.

5. Osborne, M. F., R. A. Lorenz, J. L. Collins, J. R. Travis, C. S. Webster, and T. Nakamura, "Data Summary Report for Fission Product Release Test VI-4," NUREG/CR-5481 (ORNL/TM-11400), January 1991.

6. Osborne, M. F., R. A. Lorenz, J. R. Travis, C. S. Webster, and J. L. Collins. "Data Summary Report for Fission Product Release Test VI-5," ORNL/CR-5668 (ORNL/TM-11743), October 1991.

7. Osborne, M. F., R. A. Lorenz, J. R. Travis, C. S. Webster, and C. S. Lee, "Preliminary Results from ORNL Fission Product Release Test VI-6," ORNL/NRC/LTR-91/19 (draft), September 1991.

8. Osborne, M. F., and R. A. Lorenz, "ORNL Studies of Fission Product Release Under LWR Accident Conditions," *Nuclear Safety* 33(3):344–65, July–Sept. 1992.

9. Osborne, M. F., and R. A. Lorenz, "Fission Product Release at Severe Accident Conditions: FY 1989 Program Plan," ORNL/NRC/LTR-89/2, April 1989.

10. Lorenz, R. A., J. L. Collins, and S. R. Manning, "Fission Product Release from Simulated LWR Fuel," NUREG/CR-0274 (ORNL/TM-154), October 1978.

11. Albrecht, H., "Freisetzung von Spalt- und Aktivierungsprodukten beim LWR-Kernschmelzen: Abschlussbericht des SASCHA-Programmes (Translation: Release of Fission and Activation Products During LWR Core Melting: Final Report of the SASCHA Program)," Report KfK 4264, Kernforschungszentrum Karlsruhe, Germany, June 1987.

12. Osborne, M. F., J. L. Collins, P. A. Haas, R. A. Lorenz, J. R. Travis, and C. S. Webster, "Design and Final Safety Analysis Report for Vertical Furnace Fission Product Release Apparatus in Hot Cell B, Building 4501," NUREG/CR-4332, ORNL/TM-9720, March 1986.

13. Lorenz, R. A., and M. F. Osborne, "A Summary of ORNL Fission Product Release Tests with Recommended Release Rates and Diffusion Coefficients," NUREG/CR-6261, ORNL/TM-12801, draft December 1994, in publication.

14. Pasupathi, V., L. M. Lowry, and M. C. Matthews, "Postirradiation Examination of Fuel Rods from the Monticello Reactor," BCL-585-82-2, June 1982.

15. Croff, A. G., "ORIGEN2 — A Revised and Updated Version of the Oak Ridge Isotope Generation and Depletion Code," ORNL-5621, July 1980.

16. Lorenz, R. A., et al., Prompt Release of Fission Products from Zircaloy-Clad $UO_2$ Fuels, Section 1 in "Nuclear Safety Program Annual Progress Report for the Period Ending December 31, 1967," ORNL-4228, April 1968.

# References

17. Collins, J. L., M. F. Osborne, R. A. Lorenz, and A. P. Malinauskas, "Fission Product Iodine and Cesium Release Behavior Under Severe LWR Accident Conditions," *Nucl. Technol.* 81(10):78–94 (1987).

18. Kuhlman, M. R., D. J. Lehmicke, and R. O. Meyer, "CORSOR User's Manual," NUREG/CR-4173 (BMI-2122), March 1985.

19. Toshiyuki Yamashita, "Steam Oxidation of Zircaloy Cladding in the ORNL Fission Product Release Tests," NUREG/CR-4777 (ORNL/TM-10272), March 1988.

20. M. F. Osborne, R. A. Lorenz, and J. L. Collins, "Atmospheric Effects on Fission Product Behavior at Severe Accident Conditions," in *Proc. Am. Nucl. Soc. Int'l. Top. Mtg. on the Safety of Thermal Reactors*, Portland, OR, July 21–25, 1991.

21. M. F. Osborne and R. A. Lorenz, "Results of ORNL VI Series Fission Product Release Tests," in *Proceedings of Twentieth Water Reactor Safety Information Meeting*, Bethesda, MD, October 21–23, 1992.

## INTERNAL DISTRIBUTION

| | | | | |
|---|---|---|---|---|
| 1. | K. K. Anderson | 20. | J. C. Rudolph |
| 2. | F. Barrera | 21. | R. R. Shoun |
| 3-7. | E. C. Beahm | 22. | B. B. Spencer |
| 8. | A. Boatman | 23. | R. P. Taleyarkhan |
| 9. | M. W. Burden | 24. | J. R. Travis |
| 10. | C. W. Chase | 25. | R. J. Weaver |
| 11. | J. L. Collins | 26. | C. S. Webster |
| 12. | T. A. Dillow | 27. | A. L. Wright |
| 13. | B. Z. Egan | 28. | Central Research Library |
| 14. | W. A. Gabbard | 29. | ORNL–Y-12 Technical Library |
| 15. | S. R. Greene | | Document Reference Section |
| 16. | D. D. Lee | 30-31. | Laboratory Records |
| 17. | A. P. Malinauskas | 32. | Laboratory Records, ORNL RC |
| 18. | L. E. McNeese | 33. | ORNL Patent Section |
| 19. | G. W. Parker | | |

## EXTERNAL DISTRIBUTION

34. Office of Assistant Manager for Energy Research and Development, ORO-DOE, P.O. Box 2001, Oak Ridge, TN 37831

35. Director, Division of Reactor Safety Research, U.S. Nuclear Regulatory Commission, Washington, DC 20555

36-37. Office of Scientific and Technical Information, P.O. Box 2001, Oak Ridge, TN 37831

38. B. Andre, Centre d'Etudes Nucleáires de Grenoble, DTP/SECC, 17 Rue des Martyrs, 38054 Grenoble Cedex 9, France

39. J. Bagues, Consejo de Seguridad Nuckan, SOR Angela de la Cruz No 3, Madrid 28056, Spain

40-41. A. Behbahani, Accident Evaluation Branch, U.S. Nuclear Regulatory Commission, Mail Stop T-10-K-8, Washington, DC 20555

42. N. Bixler, Sandia National Laboratory, P.O. Box 5800, Albuquerque, NM 87185

43. B. R. Bowsher, AEA Technology, Winfrith, Dorchester, Dorset DT2 8DH, United Kingdom

44. K. J. Brinkman, Reactor Centrum Nederland, 1755 ZG Petten, The Netherlands

45. M. L. Brown, 15 Barrock St., Thurso Caithness, Scotland KW14 7DB

46. I. Catton, University of California Los Angeles, Nuclear Energy Laboratory, 405 Hilgard Avenue, Los Angeles, CA 90024

47. D. S. Cox, Chalk River Laboratories, Chalk River, Ontario, Canada K0J 1J0

48. S. Hagen, Bau 601, Kernforschungszentrum Karlsruhe, Postface 3640, D7500 Karlsruhe 1, Germany

49. R. J. Hammersley, Fauske and Associates, Inc., 16WD70 West 83rd Street, Burr Ridge, IL 60521

50. R. R. Hobbins, P.O. Box 971, Wilson, WY 83014

51. F. C. Inglesias, AECL, Chalk River Nuclear Laboratories, Chalk River, Ontario, KOJ 1JO, Canada

52. S. Kinnersly, UKAEA, Winfrith, Dorchester DT2-8DH, Dorset, England

53. H. K. Lee, Spent Fuel Storage and Disposal Technology Section, Korea Advanced Energy Research Institute, P.O. Office Box 7, Dae-Danji Choong-Nam, Republic of Korea

54. R. Y. Lee, U.S. Nuclear Regulatory Commission, Office of Nuclear Regulatory Research, Mail Stop T-10-K-8, Washington, DC 20555

55. J. Leveque, Cadarache Center for Nuclear Studies, F-13108 Saint Paul-Lez Durance Cedex, France
56. B. J. Lewis, Centre d'Etudes Nucleáires de Grenoble, DTP/SECC, 17 Rue des Martyrs, 38054 Grenoble Cedex 9, France
57. Y. Y. Liu, Argonne National Laboratory, 9700 South Cass Ave., Argonne, IL 60439
58. D. Lorenz, Rt. 3, Box 314-AA, Oliver Springs, TN 37840
59. T. Nakamura, DRS/SEMAR/LPA/JAERI, CEN Cadarache, 13108 St. Paul-lez-Durance, France
60. L. A. Neimark, Argonne National Laboratory, 9700 South Cass Ave., Argonne, IL 60439
61. A. Nichols, Technology Division, AEE Winfrith, Dorchester, Dorset, England
62. K. S. Norwood, Nuclear Electric plc, Bridgwater Road, Bedminister Down, Bristol BS13 8AN, England
63-67. M. Osborne, 123 Baltimore Drive, Oak Ridge, TN 37830
68. D. J. Osetek, Los Alamos Technical Associates, Inc., 2400 Louisiana Blvd. N.E., Building 1, Suite 400, Albuquerque, NM 87110.
69. R. L. Palla, Jr., U.S. Nuclear Regulatory Commission, Office of Nuclear Regulatory Research, OWFN 10 E 4, Washington, DC 20555
70. D. A. Petti, EG&G Idaho, Inc., P.O. Box 1625, Idaho Falls, ID 83401
71. T. Pratt, Brookhaven National Laboratory, 130 BNL, Upton, NY 11973
72. K. O. Reil, Sandia National Laboratory, P.O. Box 5800, Albuquerque, NM 87185
73. J. Rest, Argonne National Laboratory, 9700 South Cass Ave., Argonne, IL 60439
74. L. A. Simpson, Whiteshell Laboratories AECL Research, Reactor Safety Research Division, Pinawa, Manitoba, Canada ROE 1L0
75. L. Soffer, U.S. Nuclear Regulatory Commission, Office of Nuclear Reactor Regulation, Mail Stop T-10-K-8, Washington, DC 20555
76. K. Y. Suh, Fauske & Associates, Inc., 16W070 West 83rd St., Burr Ridge, IL 60521
77. Kenji Takumi, Nuclear Power Engineering Center, Fujitakanko Building, 17-1, 3-Chrome, Toranomon, Minato-Ku, Tokyo 105, Japan
78. A. C. Thadani, U.S. Nuclear Regulatory Commission, Office of Nuclear Reactor Regulation, OWFN 8E2, Washington, DC 20555
79. S. Thompson, Sandia National Laboratory, P.O. Box 5800, Albuquerque, NM 87185
80. Y.C. Tong, Institute of Nuclear Energy Research, P.O. Box 3-6, Lung-Tan, Taiwan, Republic of China
81. P. Vaisnys, VATESI, Gediminis Prospect 36, Vilnius, Lithuania
82. K. Washington, Sandia National Laboratory, P.O. Box 5800, Albuquerque, NM 87185
83. D. Williams, UKAEA, Winfrith, Dorchester DT2-8DH, Dorset, England
84. S. J. Wisbey, B.220, AERE Harwell, Didcot, Oxon OX11 ORA, United Kingdom
85. J. W. Wolfe, Westinghouse Bettis Atomic Laboratory, P.O. Box 79, ZAP 34N, West Mifflin, PA 15122
86. T. Yamashita, Nuclear Fuel Chemistry Laboratory, Department of Chemistry, Japan Atomic Energy Research Institute, Tokai-mura, Naka-gun, Ibaraki-ken, 319-11, Japan
87-176. Given distribution as shown in Category R3 (NTIS – 10)

2. TITLE AND SUBTITLE

Data Summary Report for Fission Product Release Test VI-7

3. DATE REPORT PUBLISHED

| MONTH | YEAR |
|---|---|
| May | 1995 |

4. FIN OR GRANT NUMBER

L2250

5. AUTHOR(S)

M. F. Osborne, R. A. Lorenz, J. R. Travis, J. L. Collins, and
C. S. Webster

6. TYPE OF REPORT

Technical

7. PERIOD COVERED *(Inclusive Dates·*

8. PERFORMING ORGANIZATION — NAME AND ADDRESS *(If NRC, provide Division, Office or Region, U.S. Nuclear Regulatory Commission, and mailing address; if contractor, provide name and mailing address.)*

Oak Ridge National Laboratory
Martin Marietta Energy Systems, Inc.
P.O. Box 2008
Oak Ridge, Tennessee 37831-6221

9. SPONSORING ORGANIZATION — NAME AND ADDRESS *(If NRC, type "Same as above"; if contractor, provide NRC Division, Office or Region, U.S. Nuclear Regulatory Commission, and mailing address.)*

Division of Systems Research
Office of Nuclear Regulatory Research
U. S. Nuclear Regulatory Commission
Washington, D. C. 20555

10. SUPPLEMENTARY NOTES

11. ABSTRACT *(200 words or less)*

Test VI-7 was the final test in the VI series conducted in the vertical furnace. The fuel specimen was a 15.2-cm-long section of a fuel rod from the Monticello boiling water reactor (BWR). The fuel had experienced a burnup of ~40 Mwd/kg U. It was heated in an induction furnace for successive 20-min periods at 2000 and 2300 K in a moist air-helium atmosphere.

Integral releases were 69% for 85Kr, 52% for $^{125}$Sb, 71% for both $^{134}$Cs and $^{137}$Cs, and 0.04% for $^{154}$Eu. For the non-gamma-emitting species, release values for 42% for I, 4.1% for Ba, 5.3% for Mo, and 1.2% for Sr were determined. The total mass released from the furnace to the collection system, including fission products, fuel, and structural materials, was 0.89 g, with 37% being collected on the thermal gradient tubes and 63% downstream on filters. Posttest examination of the fuel specimen indicated that most of the cladding was completely oxidized to $ZrO_2$, but that oxidation was not quite complete at the upper end. The release behaviors for the most volatile elements, Kr and Cs, were in good agreement with the ORNL-Booth Model.

12. KEY WORDS/DESCRIPTORS *(List words or phrases that will assist researchers in locating the report.)*

Fission product
Fission product release
Fuel damage

13. AVAILABILITY STATEMENT

Unlimited

14. SECURITY CLASSIFICATION

*(This Page)*

Unclassified

*(This Report)*

Unclassified

15. NUMBER OF PAGES

16. PRICE